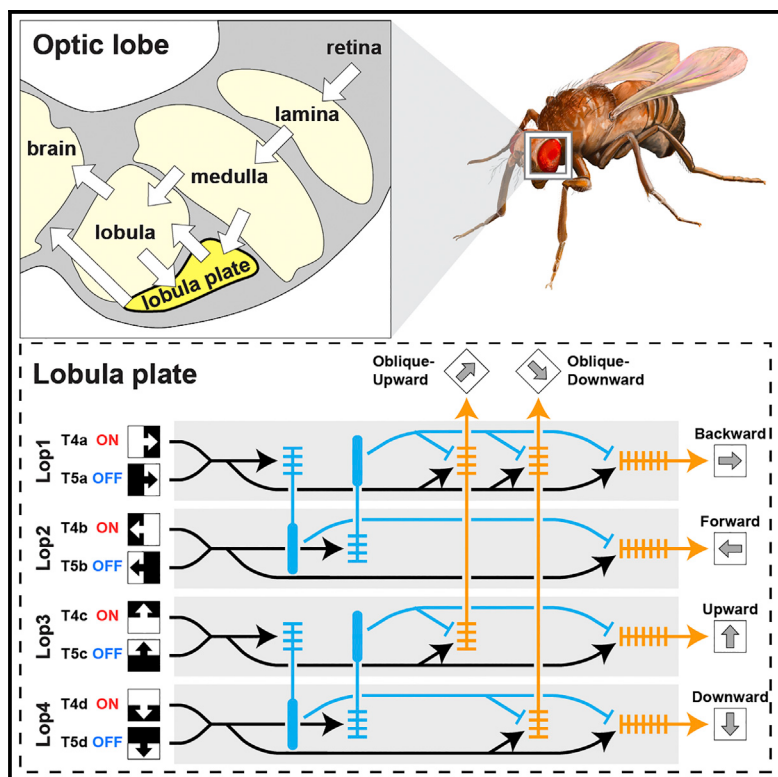


Neuronal circuits integrating visual motion information in *Drosophila melanogaster*

Graphical abstract



Authors

Kazunori Shinomiya, Aljoscha Nern,
Ian A. Meinertzhagen,
Stephen M. Plaza, Michael B. Reiser

Correspondence

kshinomiya@flatironinstitute.org (K.S.),
reiserm@janelia.hhmi.org (M.B.R.)

In brief

Shinomiya et al. report the comprehensive identification of neurons in the *Drosophila melanogaster* lobula plate that receive inputs from the directionally selective T4 and T5 cells, using a reconstruction of 3D electron microscopy data. The two pathways share common synaptic partners, and multidirectional motion signals are integrated to encode new directions.

Highlights

- EM reconstruction of lobula plate neurons integrating ON- and OFF-motion pathways
- Revealed core circuit motif of motion processing in each lobula plate layer
- Discovered novel neuron types integrating vertical and horizontal motions
- Substantial motion information flows from the lobula plate to the lobula



Article

Neuronal circuits integrating visual motion information in *Drosophila melanogaster*

Kazunori Shinomiya,^{1,3,6,*} Aljoscha Nern,¹ Ian A. Meinertzhagen,^{1,2} Stephen M. Plaza,^{1,4} and Michael B. Reiser^{1,5,*}

¹Janelia Research Campus, Howard Hughes Medical Institute, 19700 Helix Drive, Ashburn, VA 20147, USA

²Department of Psychology and Neuroscience, Dalhousie University, 1355 Oxford Street, Halifax, NS B3H 4R2, Canada

³Present address: Center for Computational Neuroscience, Flatiron Institute, Simons Foundation, 160 Fifth Avenue, New York, NY 10010, USA

⁴Present address: Meta, 1 Hacker Way, Menlo Park, CA 94025, USA

⁵Twitter: @MichaelBReiser

⁶Lead contact

*Correspondence: kshinomiya@flatironinstitute.org (K.S.), reiserm@janelia.hhmi.org (M.B.R.)

<https://doi.org/10.1016/j.cub.2022.06.061>

SUMMARY

The detection of visual motion enables sophisticated animal navigation, and studies on flies have provided profound insights into the cellular and circuit bases of this neural computation. The fly's directionally selective T4 and T5 neurons encode ON and OFF motion, respectively. Their axons terminate in one of the four retinotopic layers in the lobula plate, where each layer encodes one of the four directions of motion. Although the input circuitry of the directionally selective neurons has been studied in detail, the synaptic connectivity of circuits integrating T4/T5 motion signals is largely unknown. Here, we report a 3D electron microscopy reconstruction, wherein we comprehensively identified T4/T5's synaptic partners in the lobula plate, revealing a diverse set of new cell types and attributing new connectivity patterns to the known cell types. Our reconstruction explains how the ON- and OFF-motion pathways converge. T4 and T5 cells that project to the same layer connect to common synaptic partners and comprise a core motif together with bilayer interneurons, detailing the circuit basis for computing motion opponency. We discovered pathways that likely encode new directions of motion by integrating vertical and horizontal motion signals from upstream T4/T5 neurons. Finally, we identify substantial projections into the lobula, extending the known motion pathways and suggesting that directionally selective signals shape feature detection there. The circuits we describe enrich the anatomical basis for experimental and computations analyses of motion vision and bring us closer to understanding complete sensory-motor pathways.

INTRODUCTION

Flying flies react to complex visual stimuli with acrobatic maneuvers in a matter of milliseconds,¹ which has inspired many to use the *Drosophila melanogaster* visual system to uncover circuit mechanisms of many neural computations.^{2–9} Genetic driver lines enable studies of these computations,^{10–14} often testing circuit hypotheses suggested by connectomes based on three-dimensional electron microscopy (3D-EM). The fly optic lobe has four major neuropils (lamina, medulla, lobula, and lobula plate; Figure 1A) that are characterized by neurons connecting these structures and layer patterns housing these connections. The diversity of optic lobe neuron types has been well documented using classic methods^{16,17} and more recently genetic driver lines for cell-type-specific expression.^{12,18,19}

The synaptic connectivity of neurons in the lamina, medulla, and lobula^{15,20–24} have been described by 3D-EM reconstructions. Together with functional studies, these data have revealed the detailed circuitry and likely mechanism(s) of motion detection by T4 and T5 neurons. T4 are the ON directionally selective neurons: they encode the direction of a bright edge's motion, while

none of their dendritic inputs do.²⁵ T5 are OFF directionally selective neurons that encode the direction of moving dark edges by integrating inputs onto their dendrites in the first lobula layer (Lo1).^{15,26} Both cells have four distinct subtypes, a, b, c, and d, that each project axons, retinotopically arranged, to one of the four layers of the lobula plate (Figure 1B).^{9,16}

The evolutionary origin of the lobula plate may relate to the origin of insect flight.²⁷ The neuropil is best known for containing the dendrites of the “giant” lobula plate tangential cells (LPTCs).^{17,28–31} Many of these cells encode the optic flow—the pattern of visual motion—seen by flies during flight maneuvers such as body rotations,³² suggesting that they play a key role in regulating flight behaviors. The vertical system (VS) and horizontal system (HS) cells, which have been identified in both larger flies and *Drosophila*,^{16,29} are the best-studied LPTCs. The morphology of these cells in *Drosophila* was examined using genetic single-cell labeling,³³ and the electrophysiologically measured responses of these cells to visual motion patterns match those of larger flies.^{34,35}

The 2-photon calcium imaging of T4 and T5 responses in the lobula plate⁹ has revealed that these inputs into the lobula plate



mainly respond to motion along one cardinal direction: front-to-back (Lop1), back-to-front (Lop2), upward (Lop3), and downward (Lop4), near the center of the eye. However, recent work has shown that the population of T4/T5 cells encodes a global pattern that is not consistent with these cardinal directions throughout the eye.³⁶ Anatomical and physiological data suggest a correlation between an LPTC's visual motion responses and its lobula plate layer pattern,^{29,37} although each neuron's selectivity for visual motion patterns can be influenced by network connections.^{38,39} Many details of the lobula plate circuitry have not been thoroughly investigated, with the noteworthy exception of two bilayer lobula plate-intrinsic (LPI) cells: LPi3-4 receives input in Lop3 and provides output to Lop4, whereas LPi4-3 sends signals from Lop4 to Lop3.^{16,40,41} These cells inhibit their target LPTCs in response to motion in the opposing direction, sharpening the flow-field selectivity of the tangential cells, in a computation termed "motion opponency."⁴⁰ Functional studies^{4,40,42} suggest this occurs through the integration of excitatory, cholinergic T4/T5 input and inhibitory, glutamatergic LPI inputs by LPTCs, but the synaptic connectivity proposed by this parsimonious circuit hypothesis had not been verified.

The lobula plate also houses processes of other columnar neuron types, including optic lobe-intrinsic neurons, such as Y, TmY (transmedulla Y), and Tlp (trans lobula plate) cells, which connect different optic lobe neuropils, and the LPC (lobula plate columnar), LLPC (lobula-lobula plate columnar), and LPLC (lobula plate-lobula columnar) cells, which are visual projection neurons (VPNs) into the central brain.^{4,16,43–49} Detailed connectivity information for these neurons is unknown and represents the last piece of the puzzle for the anatomical description of the motion information-processing circuit in the optic lobe. To close this gap, we reconstructed the neurons downstream of T4 and T5 in the lobula plate using a dataset imaged with focused-ion beam-aided scanning EM (FIB-SEM).^{15,50} We exhaustively identified and cataloged T4/T5 synaptic partners and investigated complete synaptic profiles of LPI cells and the HS and VS cells. In the process, we identified new cell types as important components of the motion vision pathway and attributed new connectivity patterns to the known cell types, resolving several open questions about lobula plate connectivity.

RESULTS

EM reconstruction of the synaptic partners of T4 and T5 cells in the lobula plate

Our FIB-SEM data volume^{15,50} includes large parts of the lamina, medulla, lobula, and lobula plate (Figure 1A), covering regions corresponding to the eye's equator. This volume contains many connected neurons corresponding to common retinotopic coordinates, enabling circuit reconstruction across neuropils. Medulla neurons, including Mi1, Tm1, and Tm2, relay signals to T4 in M10 and T5 in Lo1 (Figure 1A).¹⁵ The four subtypes of T4 and T5 send outputs to one of the four lobula plate layers (defined to encompass the terminals of groups of T4 and T5 cells; **STAR Methods**), where they synapse with optic lobe interneurons and neurons projecting to the central brain (Figures 1B and 1C). The major findings of our analysis are summarized in a

series of figures and data tables (Data S1, S2, and S3; see [resource availability](#) for further data availability).

Connectivity of the seed T4 and T5 cells in the lobula plate

We reconstructed and then identified many neurons in the FIB-SEM volume, focusing on T4 and T5 cells and their targets. In total, 277 T4s and 277 T5s were identified and at least partially reconstructed. Five cells of each subtype from a retinotopically overlapping region near the volume center were completely traced.¹⁵ In the previous study, we detailed the dendritic inputs of these neurons, and here, we describe the connectivity of these same 40 cells in the lobula plate. All computationally predicted synapses (**STAR Methods**) of these cells were proofread to identify their presynaptic and postsynaptic partners.

The connectivity of the inputs and outputs of the representative T4 and T5 cells in the lobula plate is summarized in Figure 2A, including all neurons connected with ≥ 5 synapses to any of the seed neurons (detailed connectivity data are in Data S1; connectivity summary for ≥ 3 synapses is in Figure S1). We found 58 putative connected neuron types (mean of ≥ 5 synapses with any T4 or T5), including 16 unidentified fragments (Figure 2A; shown in gray). 74% of these communicate with the same subtype of T4 and T5, resulting in the four clusters in the connectivity diagram, each corresponding to synapses within one lobula plate layer. One noteworthy exception is LPLC2, the only neuron found to receive inputs from all T4/T5 subtypes, corroborating the observation that this cell type integrates spatially patterned inputs to detect looming objects.⁴

How are the ON and OFF pathways integrated into the lobula plate? In nearly every case, neurons that are strongly connected to T4/T5 receive inputs from both cells but with a consistent bias for T5 (pooled across all downstream neurons: 45.4% T4 versus 54.6% T5; Figure 2B). This suggests that lobula plate neurons that primarily integrate inputs from T4 and T5 should respond to both bright and dark moving edges. However, some neurons may show differential sensitivity to dark or bright objects due to the greater percentage of inputs from T5 neurons as well as from other inputs. For example, LPLC2 responds more strongly to dark looming stimuli,⁴ despite substantial, though T5-biased, inputs from both cells (Figure 2B).

In mapping computational models onto the circuitry of the motion pathway, the T4/T5 axons are treated as output structures.⁴⁰ We find that T4 and T5 axon terminals are the primarily sites of synaptic output but have some inputs: 87% of T4's and 88% of T5's lobula plate synapses are presynaptic. T5 neurons feature higher synapse counts, which is consistent with the connectivity bias for T5 inputs (Figure 2B). We find T4-T4, T5-T5, and T4-T5 connections within each layer that account for 27.8% of the total inputs to these cells (Data S1). These occur between neighboring axon terminals, and each inter-terminal connection is typically ≤ 3 synapses and are reminiscent of the within-subtype connections seen between dendrites of these cells.¹⁵ Several cell types, including Y11 and Y12, provide strong input to T4/T5 terminals (indicated in magenta, Figure 2A), but it is not known whether these neurons inhibit or excite T4 and T5. T4 and T5 neurons with more output synapses tend to have more inputs (Figure 2C). For example, T4a and T5a had more presynapses and postsynapses than the other subtypes, due

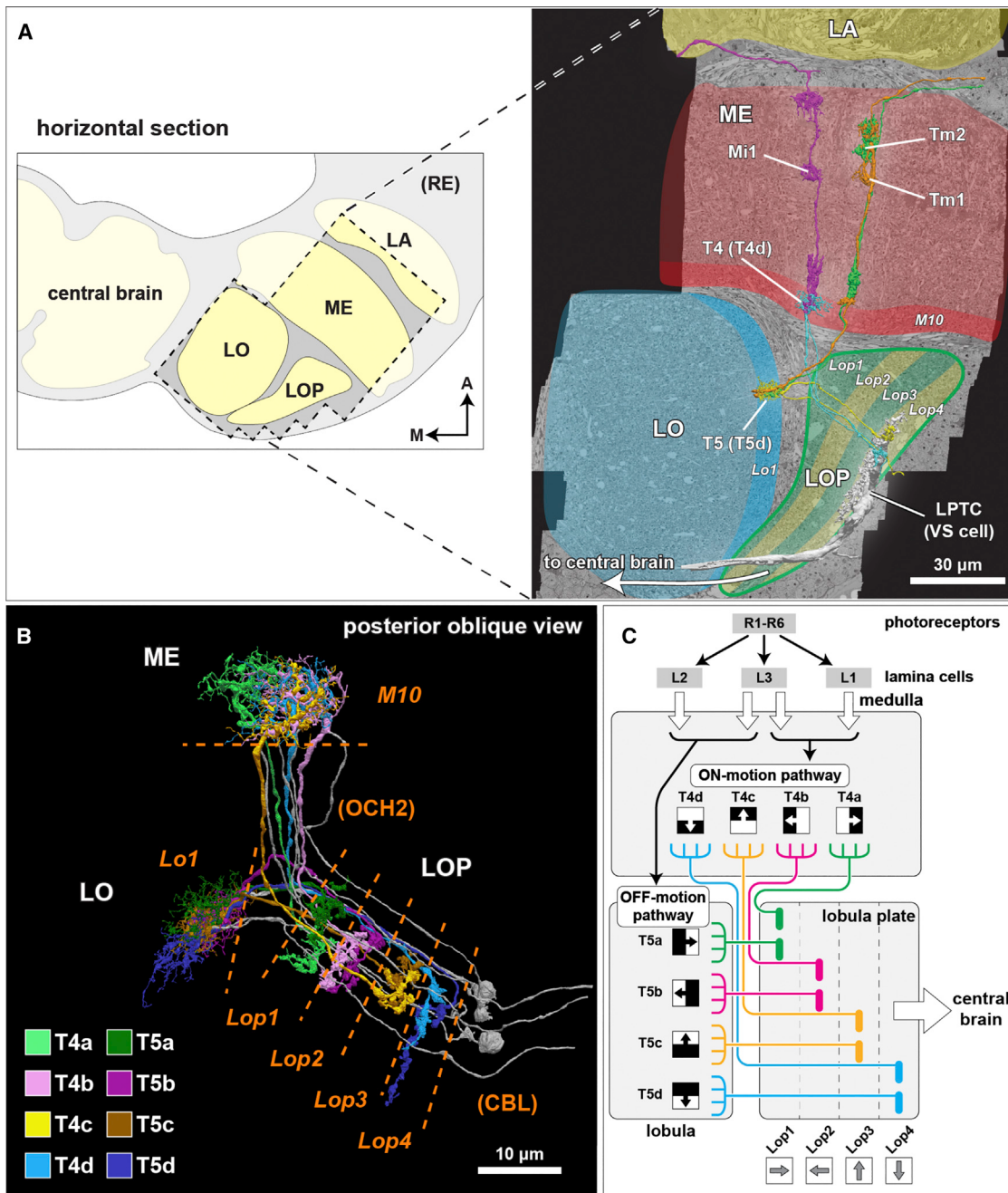


Figure 1. EM reconstruction of the synaptic partners of T4 and T5 cells in the lobula plate

(A) The optic lobe FIB-SEM dataset covers a subvolume of the medulla (ME), lobula (LO), and lobula plate (LOP), as well as the proximal part of the lamina (LA), selected to contain many connected neurons of the motion pathway. The dataset was imaged with voxel size $x = y = z = 8 \text{ nm}$, and the size of the image stack is $19,162 \times 10,657 \times 22,543$ pixels, equivalent to $153 \times 85 \times 180 \mu\text{m}$.¹⁵ In the right panel, representative neurons in the ON- and OFF-motion pathways in the medulla and the lobula, as well as a lobula plate tangential cell (VS cell) are shown (panel was adapted from Shinomiya et al.¹⁵). M, medial; A, anterior.

(B) Subtypes of the T4 and T5 cells. The T4 cells receive inputs onto their dendrites in medulla layer 10 (M10), and T5 neurons receive dendritic input in lobula layer 1 (Lo1). Both cell types project through the non-synaptic second optic chiasm (OCH2) and stratify into the four layers of the lobula plate (Lop1–Lop4). The cell bodies are located at the cell body layer (CBL) in the lobula plate cortex. The cell bodies and the cell body fibers are shown in gray, while some cell bodies are not shown.

(C) A schematic diagram of the motion circuit. Local luminance is detected by the photoreceptors R1–R6 in the retina. The signals are relayed to the lamina cells (L1, L2, and L3), which send outputs to various columnar cells in the medulla (not detailed here). The 4th order T4 and T5 neurons integrate inputs from the ON- and OFF-motion-pathway neurons, respectively, and project to the lobula plate. The four subtypes (a, b, c, and d) detect visual motion in the front-to-back, back-to-front, upward, and downward directions, respectively, and project axons to the corresponding lobula plate layer where these directionally selective signals are integrated by lobula plate neurons.

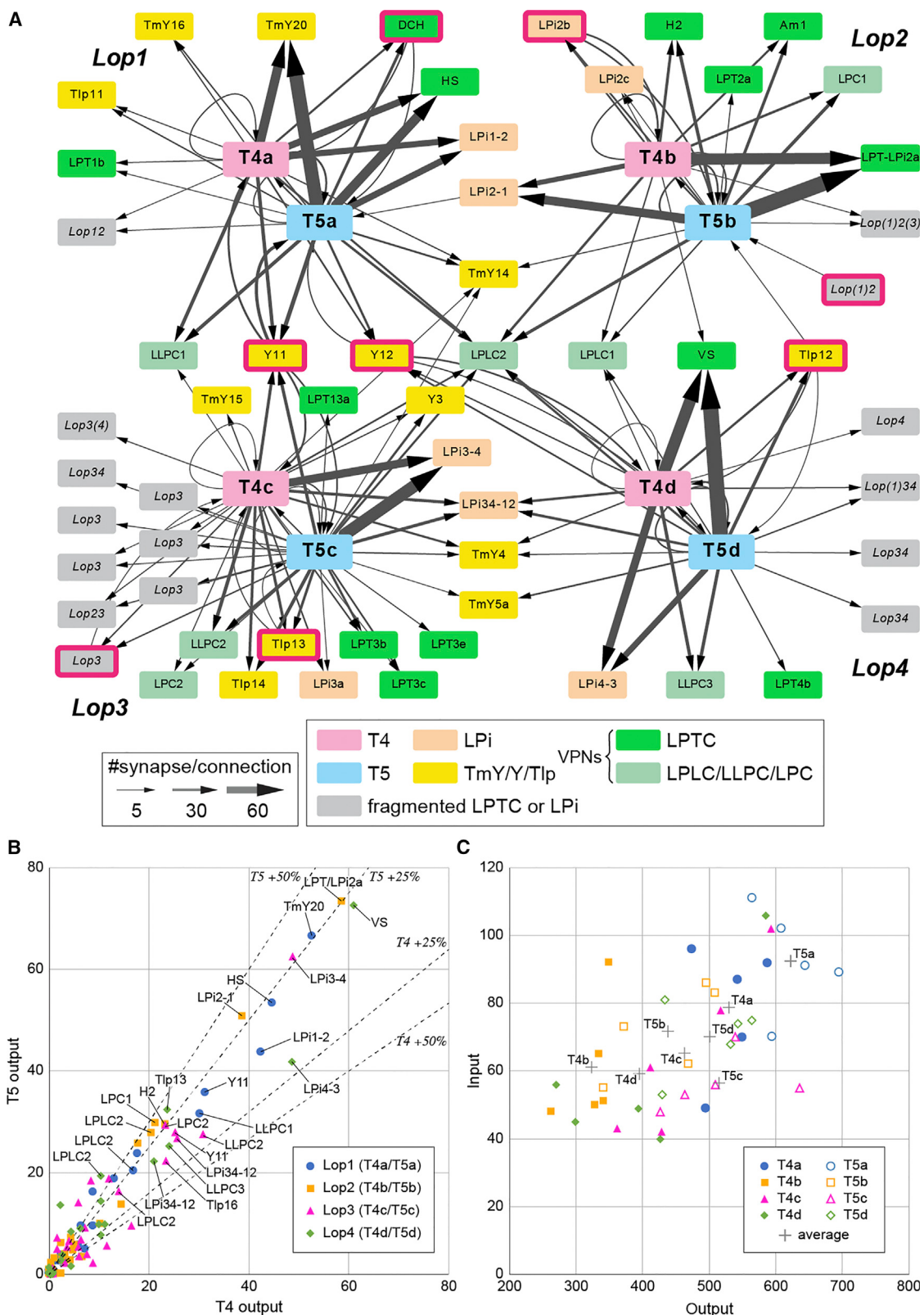


Figure 2. Connectivity of the seed T4 and T5 cells in the lobula plate

(A) The inputs and outputs of representative T4 and T5 cells (five cells per each subtype; see text for details and also [Data S1](#)) in the lobula plate were comprehensively identified. The input and output cells were grouped by the cell type, and the inputs and outputs corresponding to a mean of more than five

(legend continued on next page)

to strong connections with several Lop1 neurons, including TmY20, HS, and LPi1-2 cells (Figure 2A; Data S1).

T4 and T5 provide strong inputs to diverse VPNs, including many tangential cells (identified cells named and indicated in green; Figure 2A). The connectivity of the well-known HS and VS cells^{29,33} is described in Figure 3. Small-field VPN types (LPC, LLPC, and LPLC cells)^{43,45,48,49} are also found with substantial T4/T5 inputs in each layer, and the morphology of connected VPNs is shown in Figure 5. T4 and T5 cells synapse onto bilayer LPi cells in each layer, which are further explored in Figure 4. We also identified many connections between T4/T5 neurons and other optic lobe-intrinsic neurons, such as the TmY, Y, and Tlp cells (morphology shown in Figure 6) that interconnect different neuropils. For most newly described optic lobe-intrinsic cell types, we provide light microscopy (LM) images as additional validation (Figures S2 and S3). We conclude with a summary of the core connectivity motifs at this output stage of the visual motion pathway (Figure 7).

Synaptic connections of the horizontal system (HS) and vertical system (VS) lobula plate tangential cells

The HS and VS cells have been extensively studied^{32–35,53} and are major T4/T5 targets in their respective layers (Figure 2A). In Lop1, T4a and T5a provide strong inputs to the HS cells (T4a, mean of 44.6 synapses; T5a, mean of 53.4 synapses; Data S1). Each lobula plate houses 3 cells, HSN, HSE, and HSS (north, equatorial, and south).³³ In our imaged volume, we find identifiable fragments of all three cells (Figures 3A and 3B), with dendrites that are almost purely postsynaptic. Based on the computational predictions, HSN, HSE, and HSS had 6,151, 4,514, and 2,066 postsynaptic densities and 7, 2, and 3 presynaptic T-bars, respectively, with most of the inputs supplied by T4a and T5a (Figure 3F).

In Lop4, the VS cells receive a large fraction of T4d and T5d's synaptic outputs (Figures 2A and 2B). We identified 10 VS or VS-like cells in Lop4 (Figures 3C and 3D), exceeding the expected number of VS cells in *Drosophila* based on earlier genetic labeling studies³³ but consistent with the number in larger flies^{31,54,55} and a recent reconstruction in *Drosophila*.³⁷ These 10 cells have many common features: primary dendritic processes in Lop4 that are predominantly postsynaptic (typically >95% of the total synapses) and simple connectivity profiles, with ~90% of the inputs supplied by T4d, T5d, and LPi3-4 (Figure 3F; Video S1). Four of the 10 VS and VS-like cells also have dendritic branches in Lop2 (Figure 3D). VS cells with dendritic arbors outside Lop4

have been previously described.^{37,56} By integrating directionally selective inputs in other layers, these neurons should incorporate regional horizontal motion that accompanies body and head rotation around certain axes.^{32,56,57}

HS and VS cells are connected with a very small set of cell types in the lobula plate, outlining minimal circuit elements that could participate in the nonlinear summation of dendritic inputs.⁵⁸ To quantify the input connectivity of these large neurons, we selected small (≤ 300 postsynaptic sites) branches of HS cells (one each from HSN and HSS) and VS cells (two Lop4 branches and one Lop2 branch; each from different cells) and proofread all synaptic sites. Figure 3E shows an HS branch and a Lop4 VS branch, and Video S1 shows a VS branch and its input neurons. The summary of these connectivity analyses (Figure 3F) shows that ~80% of the inputs are supplied by T4/T5. The HS (Lop1), VS (Lop4), and VS (Lop2) branches receive 7.14%, 18.9%, and 10.7% of input synapses from bilayer LPi cells, respectively (Figure 3F; Data S2). Intriguingly, the Lop2 VS branch receives inputs mainly from T4b, T5b, and LPi1-2 cells, suggesting that it indeed receives back-to-front local motion signals.

How are the inputs from T4, T5, and LPi neurons organized onto the dendrites of these LPTCs? The spatial distribution of T4a, T5a, and LPi2-1 inputs onto HS cells features synapses throughout the thickness of Lop1 without any apparent organization or substructure (Figures S4A and S4A'). Likewise, VS and their input neurons display a patchy but mostly uniform synapse distribution in Lop4, whereas the Lop2 VS branch synapses are only found in the distal half of the layer (Figures S4B and S4B'). The individual input synapses from T4, T5, and bilayer LPi onto individual HS and VS branches also feature a patchy distribution but with no obvious pattern in any of the three layers (Figure S5, fragments same as those analyzed in Figure 3; Data S2). Overall, the connectivity between T4/T5, LPi, and the giant LPTCs is very similar across these layers (Figures 3E and 3F). This relatively simple connectivity structure strongly supports the expectations of the functional studies of HS and VS—they mainly integrate inputs from directionally selective T4/T5 cells that are further sharpened by motion opponent inputs from LPi neurons.⁴⁰

Connectivity of the bilayer lobula plate-intrinsic (LPi) cells

We identified four bilayer LPi neuron types as major T4/T5 targets (Figure 2A). A previous study described LPi3-4 and LPi4-3

synapses per T4 or T5 cell are shown in the diagram (see Figure S1 for the same diagram but with the threshold lowered to three synapses per T4 or T5). The thickness of the arrows indicates the average number of synapses per T4 or T5 cell. Each rectangle indicates a cell type: colored rectangles correspond to uniquely identified cells, and gray rectangles represent neurons we could not uniquely identify due to incomplete reconstruction. For unidentified neurons, the main innervated layers are shown in italic letters. For example, *Lop(1)34* means that the fragment has major arbors in Lop3 and Lop4 and minor arbors in Lop1. Several unidentified neuron fragments share a common designation (e.g., Lop3) but are likely to represent independent neurons (so far as can be determined within the limited data volume). LPi are lobula-plate-intrinsic cells; the TmY/Y/Tlp neurons connect the optic lobe neuropils, and LPTC and LPLC/LLPC/LPC cells are visual projection neurons (VPNs) that send outputs to the central brain. T4 and T5 receive far fewer synaptic inputs in the lobula plate than they provide output synapses. The cell types with more than five input synapses to T4 or T5 are highlighted with magenta frames.

(B) Average numbers of output synapses from single T4 and T5 per postsynaptic cell type. Neurons are color coded by the layer where they receive inputs from T4 and T5. Generally, the outputs from T4 and T5 (and therefore inputs to their target neurons) are approximately evenly integrated by the postsynaptic cells, with a slight bias for T5. All the named neurons receiving more than an average of 20 synapses from both T4 and T5 are labeled (LPLC2 is labeled for all four layers). The dashed lines indicate a 25% and 50% difference from equal numbers of output from T4 and T5 to any target cell type.

(C) Total numbers of input and output synapses of the representative T4 and T5 cells. Autapses (self-synapses) and synaptic contacts with glia are excluded from this quantification. Averaged synapse numbers of each cell type (five individual neurons per each cell type) are indicated as gray crosses.

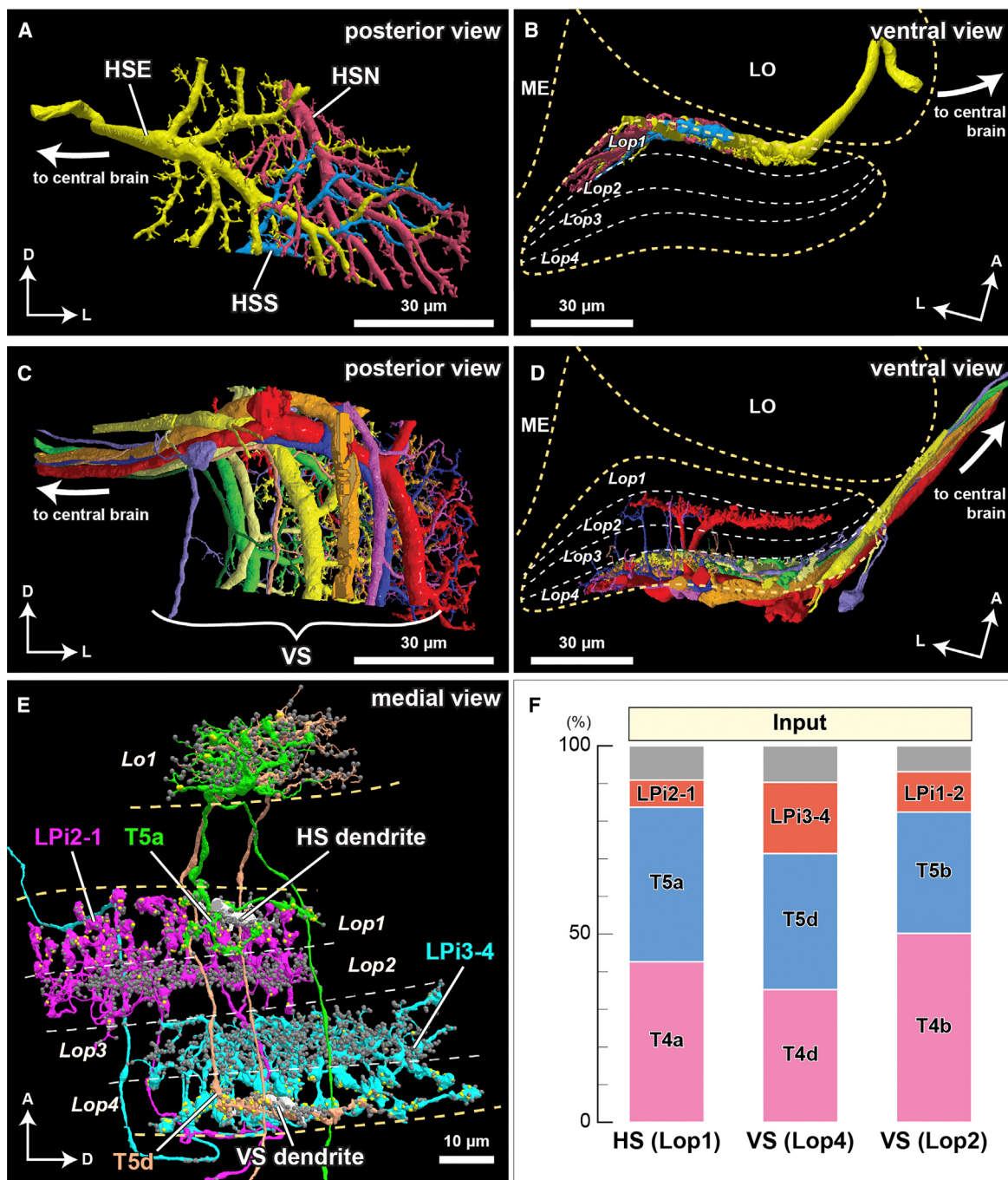


Figure 3. Synaptic connections of the horizontal system (HS) and vertical system (VS) lobula plate tangential cells

(A and B) The three HS cells (HSN, HSE, and HSS) occupy Lop1, the first layer of the lobula plate. Collectively, the dendrites of these neurons span Lop1 and overlap in the region of the lobula plate within our data volume but are cut off at the edges of the volume. (A) Posterior view; (B) ventral view.

(C and D) The ten identified VS cells in our data volume. All have postsynaptic terminals in Lop4, whereas four of them also have branches in Lop2. (C) Posterior view; (D) ventral view.

(E) Examples of major input neurons to the HS and VS cells in the lobula plate. Single-dendritic arbors (length ~20 μm) of one HS cell and one VS cell are shown in white. HS dendrites primarily receive input from the T4a, T5a, and LPi2-1 cells in Lop1, whereas VS dendrites in Lop4 primarily receive input from the T4d, T5d, and LPi3-4 cells. The T4 terminals are not shown to minimize clutter. Yellow and gray dots represent presynaptic and postsynaptic sites, respectively. The synapse distributions of HS, VS, and their input cells in the lobula plate are shown in more detail in Figures S4 and S5; inputs to a VS cell are illustrated in Video S1.

(legend continued on next page)

and speculated about the existence of all four types.⁴⁰ Here, we have reconstructed and identified LPi1-2 and LPi2-1 that bridge Lop1 and Lop2, confirming these predictions, although we are unable to describe their complete morphology. We found a strong candidate for LPi1-2 using LM (Figure S2A), which suggests that LPi1-2, and perhaps also LPi2-1, may be considerably larger than LPi3-4 and LPi4-3. Confirming this proposal will require extensive reconstruction in a larger EM volume. All four LPi neuron types innervate neighboring layers, with a stereotypic synapse distribution (Figure 4, left). Each cell type has postsynaptic sites in one layer and presynaptic T-bars in the adjacent layer. At least 2/3 of the inputs are from layer-specific T4/T5 cells, whereas the outputs are shared by many neuron types (Figure 4, right; Data S3). The proportion of output synapses relative to all synaptic connections is very similar in LPi1-2, LPi2-1, and LPi4-3 and is close to 50%, whereas this number is lower in LPi3-4 (Data S3), implicating functional or developmental differences.

The LPi3-4 and LPi4-3 cells are glutamatergic,^{40,46} and these cells provide directionally selective inhibition to target neurons.^{40,42} Based on their similar morphology and connectivity, LPi1-2 and LPi2-1 are also likely inhibitory. This small circuit supports the Mauss et al.⁴⁰ mechanism: bilayer LPi cells integrate T4/T5 inputs in one layer and inhibit postsynaptic neurons integrating oppositely tuned T4/T5 signals in the adjacent layer, implementing motion opponency. The ~1/3 of LPi inputs provided by various cells other than T4/T5 suggest that the lobula plate circuitry is more complicated, and perhaps more flexible, than the circuit models consider.

Lobula plate visual projection neurons (VPNs) that integrate T4 and T5 inputs

In addition to HS and VS cells (Figure 3), we identified other VPNs as T4/T5 targets (Figures 2 and 5). In this study, we focused on identifying and quantifying T4/T5 target neuron connectivity rather than describing the complete synaptic profiles of the VPNs.

T4 and T5 connect with columnar VPNs, smaller cells that as a population cover large parts of the lobula plate. These cells belong to three main groups (LPC, LLPC, and LPC) that are distinguished by innervation patterns in the optic lobe and axonal path to the central brain (further explained in Figure 5 legend). Based on their arbor sizes in the lobula plate and T4/T5 and LPi inputs, these cells likely respond to visual motion within small patches of the fly's field of view. We distinguished two LPC types and three LLPC types based on lobula plate layer patterns (Figures 5A–5E), in agreement with LM analyses.⁴⁹ LPC1 (Figure 5A) receives inputs from T4b and T5b. This anatomy suggests that these cells integrate back-to-front motion signals, which has been confirmed by calcium imaging.⁴⁹ LPC2 (Figure 5B) receives T4c/T5c inputs (Figure 2A) and is expected to encode upward motion. LLPC1 (Figure 5C), a VPN responsive to front-to-back visual motion,⁴⁹ has

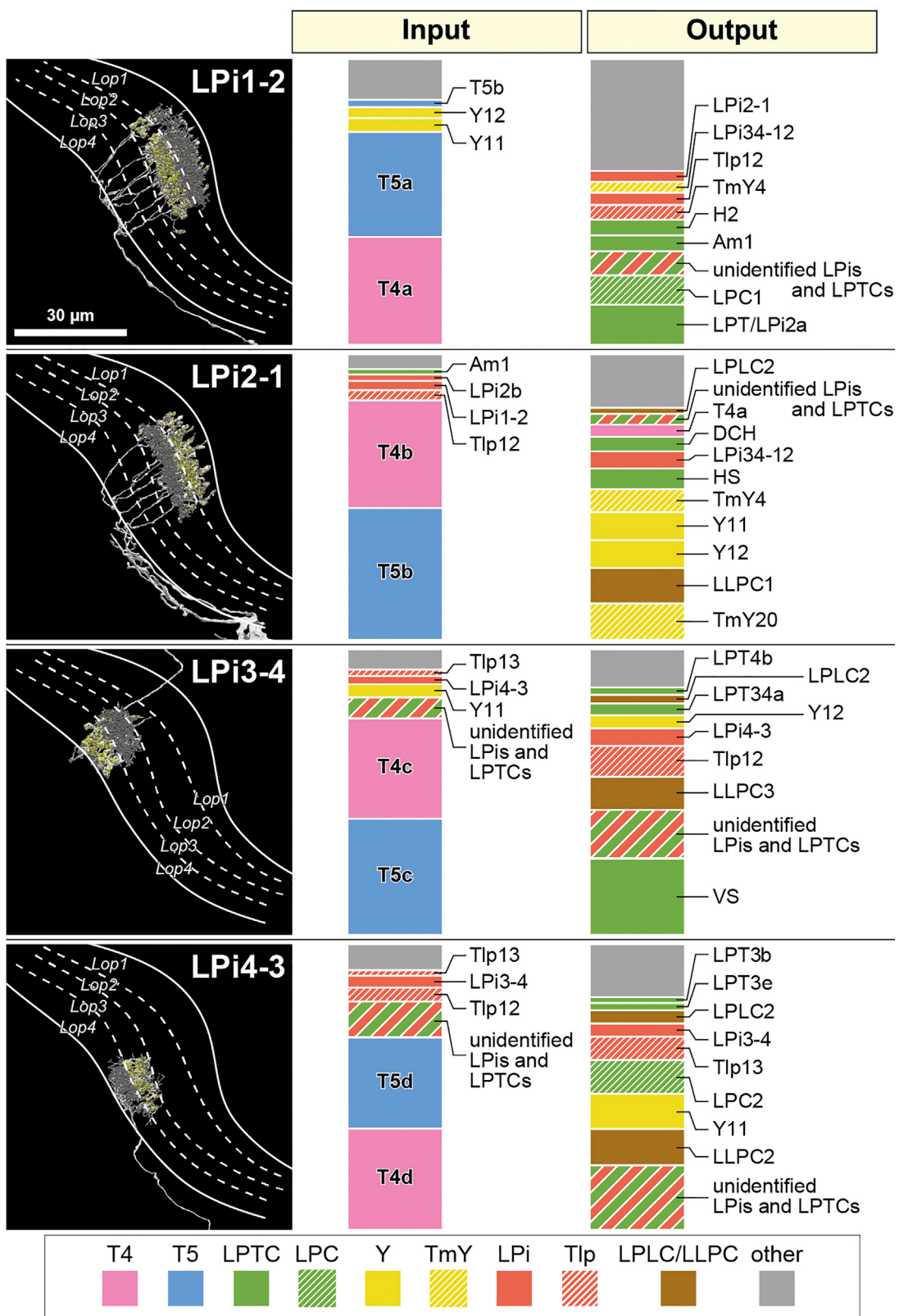
dendritic arbors in Lop1 and Lop3, with stronger T4/T5 input in Lop1 (Figure 2A). The process in the lobula appears to be mainly presynaptic (Figure 5C). LLPC2 and LLPC3 are similar cells with T4/T5 input in Lop3 and Lop4, respectively (Figures 5D and 5E). LPC1 and LPC2 cells^{43,45} are notable for receiving T4/T5 inputs in multiple lobula plate layers: T4/T5 a, b, c, and d for LPC2, in agreement with the described mechanism of looming sensitivity,⁴ and T4/T5 b and d for LPC1 (Figures 2A, 5F, and 5G).

T4 and T5 neurons connect with LPTCs, some of which we matched to known neurons, but in other cases, we name them based on their layer innervation patterns (Figures 5H–5O). As most LPTCs are morphologically unique, these cells could be matched to LM images or other EM reconstructions.^{37,59} One cell we matched based on its unique morphology is LPT13a (EM, Figure 5J; LM, Figures S2D and S2D'). The dorsal centrifugal horizontal (DCH) cell (Figure 5P) is a unique LPTC that is predominantly presynaptic to T4 and T5 (Figure 2A): 15.3% of T4a inputs and 12.7% of T5a inputs (excluding synapses between T4/T5 terminals) are from DCH, by far the largest input to T4/T5 from a single LPTC. The terminals of DCH cover the dorsal half of Lop1, whereas the homologous VCH cell covers the ventral half.^{37,52,60} The CH neurons innervate the ipsilateral inferior posterior slope in the central brain, are GABAergic,^{52,61,62} and likely inhibitory. Although we did not find VCH (due to the restricted volume), our data suggest that these two cells are the only major LPTCs that feed signals from the central brain to T4a/T5a (Data S1).

H1 is a heterolateral LPTC directly connecting both lobula plates (Figure 5Q)²⁹ and is sensitive to ipsilateral back-to-front visual motion, similar to H2.^{39,51} We found profiles that likely correspond to the proximal and distal terminals of both H1 cells. The proximal terminal is predominantly postsynaptic and confined within Lop2, whereas the putative distal terminal branch is presynapse rich, with boutons mainly in Lop1 and Lop2. The proximal terminal receives inputs from T4b and T5b (mean is ~4.8 synapses per terminal from both T4b and T5b; Figure S1). While this connection strength is lower than many T4/T5 target neurons, H1 is expected to integrate from many T4b/T5b throughout Lop2, which is consistent with the described motion preference.^{29,39,51,60} The distal terminal of H1 has limited synaptic contacts with T4 or T5 cells (only accounting for ~0.1% of H1's predicted outputs).

The H2 cell, another identifiable LPTC that is known from larger flies, has dense neuronal processes confined to Lop2 (Figure 5R), is a strong T4b/T5b target (Figure 2A), and projects to the inferior posterior slope in the contralateral brain hemisphere.^{31,52} H2 branches in Lop2 feature mixed presynaptic and postsynaptic terminals (Figure 5R, inset), as suggested by genetically driven synaptic markers.⁵² The "hemibrain" connectome dataset shows H2 as the strongest input to DCH and VCH⁴⁸ in the central brain, thus contributing to processing motion information from both eyes.

(F) Inputs to the HS and VS cells. Synapses are verified and counted for small pieces of the HS and VS arbors in the respective layers (two branches for each of HS and VS [Lop4] and one branch for VS [Lop2]). Almost 90% of the inputs to the HS and VS cell dendrites come from T4, T5, and the bilayer LPi cells. A similar input distribution is found for the VS cells' branches in the Lop2 layer, where they receive inputs from the T4b, T5b, and LPi1-2 cells. Gray indicates other, more weakly connected neurons or unidentified neuron fragments, less than 10% of the total synapses (detailed in Data S2). No output synapses were found on these branches. The scale bars are approximate, as the neurons are three-dimensionally reconstructed.



(legend on next page)

Optic lobe-intrinsic neurons that integrate T4 and T5 inputs

T4 and T5 target optic lobe-intrinsic cells other than the bilayer LPi neurons, including several types of LPi, TmY, Y, and Tlp neurons (Figure 6). We identified both known and new optic lobe-intrinsic cell types as T4/T5 targets. For most of the new cell types in this group, we further confirmed their morphology with LM matches (Figure S3).

Am1 is a single, large, amacrine-like neuron innervating the medulla, lobula, and lobula plate with tree-like arborization.^{28,50} Am1 receives inputs from T4b/T5b in Lop2 (Figures 2A and 6A) and has significant synaptic contacts with some LPTCs. The predicted synapses contain strong inputs from DCH and contralateral H1 and outputs to DCH and HS cells. Based on these connections, we expect that Am1 is inhibitory (unlikely to excite HS cells in response to ipsilateral T4b/T5b input) and participates in a bilateral circuit that integrates horizontal motion signals from both eyes^{38,39,51,63} (Figure 7C).

We find several putative LPi and LPi-like neuron types (Figures 6B–6F) that all differ from the bilayer LPi types and further illustrate the diverse neuronal composition of each layer. A large cell we tentatively named LPT/LPi2a receives the strongest inputs from T4b and T5b among all neurons in our data (Figures 2A and 6B). LPT/LPi2a has a similar but distinct morphology from the bilayer LPi2-1 cell in the lobula plate, with main branches containing presynapses and postsynapses in Lop2 with additional sparser processes in Lop1. While T4/T5 supply >80% of LPi2-1's input, they supply <50% for LPT/LPi2a, suggesting that it participates in circuits with more elaborate connectivity than the main bilayer LPis (Figure 7A). Our best candidate for an LM match is a VPN with a central brain projection (Figure S2B). LPi2b is another large Lop2 cell that appears to span the entire lobula plate, but with a more restricted layer pattern and fewer T4/T5 inputs (Figures 6C and S2C). LPi34-12 (Figures 6D and S3I) is named for its layer pattern, as it receives T4/T5 input in both Lop3 and Lop4 and has output synapses in Lop1 and Lop2 (Figure 2A). This cell likely implements an undescribed interaction between motion detected along different directions.

TmY cells have cell bodies in the medulla cell body rind and terminals in both the lobula and lobula plate (Figures 6G–6L). TmY4, TmY5a, TmY14, and TmY15 have been previously described,^{15,16,22,23} whereas TmY16 and TmY20 are reported here for the first time and confirmed with LM matches (Figures S3A and S3B). Among all T4a/T5a targets, TmY20 has the highest number of inputs (Figure 2A; Data S1). Unlike most TmY cells, the TmY20 neurite in the medulla apparently lacks synapses (reminiscent of LPi3-4, which also lacks synapses in

the medulla⁴⁰). TmY20 has mostly presynaptic terminals in lobula layers Lo5 and Lo6 (Figure 6L), suggesting that this neuron relays front-to-back motion information to lobula neurons. The other TmY cells have extensive arborizations outside the lobula plate, and a full inventory of their connectivity may be required for detailed predictions about their role in motion processing. Y cells (Figures 6M–6O) are columnar neurons with cell bodies in the rind posterior to the lobula plate that innervate the medulla, lobula, and lobula plate.¹⁶ Tlp cells (Figures 6P–6S and S3E–S3H) are similar to Y cells but lack a medulla branch. We identify one known (Y3) and two previously undescribed Y neurons (Y11 and Y12) as T4/T5 targets and confirm their morphology using LM (Figures S3C and S3D). Tlp, Y, and TmY cells all provide paths for relaying different subsets of T4/T5 outputs to the lobula (Figure 7D).

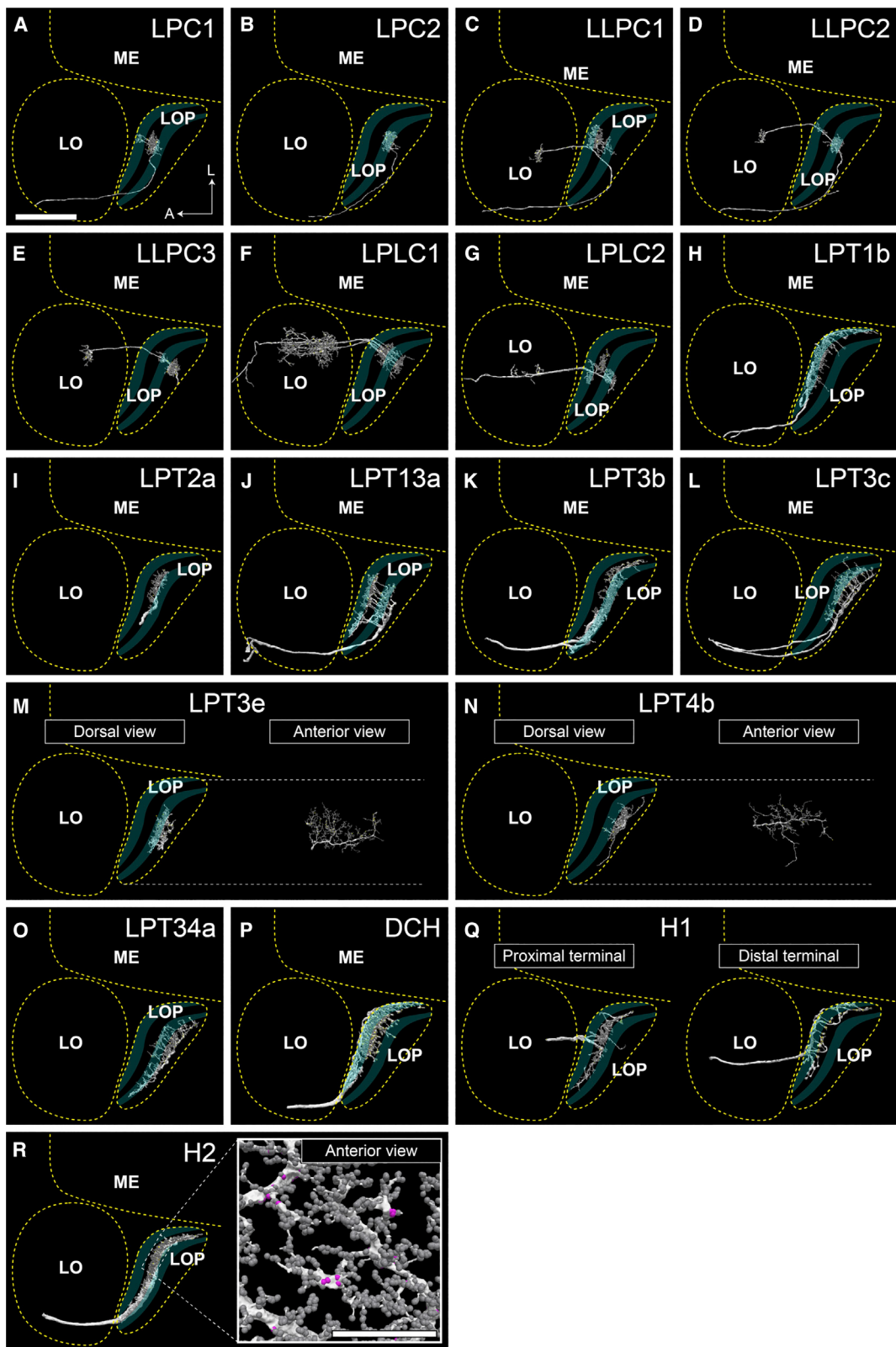
Y11 and Y12 are notable for integrating T4/T5 input from different layers: Y11 from Lop1 and Lop3 and Y12 from Lop1 and Lop4. The two cells are otherwise morphologically very similar, with boutons in the same medulla and lobula layers. Both cell types have presynaptic and postsynaptic contacts with T4 and T5 (Data S1), integrating their signals in their respective layers. Since Y11 synthesizes front-to-back (Lop1) and upward (Lop3) motion signals and Y12 combines front-to-back and downward (Lop4) motion signals, the two cells are likely to each encode a preferred motion direction in between the preferred directions of their input T4s and T5s (Figure 7B).

DISCUSSION

The giant tangential cells of the fly lobula plate have received considerable interest for decades,^{31,64,65} but the circuit description of this “final” optic lobe stage of the motion pathway has been rather incomplete. In this study, we used EM reconstructions to inventory the synaptic partners of T4 and T5 neurons with completeness unmatched by other approaches. By focusing on the neurons with an indispensable role in motion information processing—T4, T5, and the LPi neurons—we find a stunning diversity of synaptic partners in the lobula plate and establish a substantial catalog of neurons implicated in motion processing for future functional investigations. Our work reveals an elaborate architecture for processing visual motion, with several major findings: (1) all the lobula plate neurons downstream of T4 and T5 integrate from both cell types, with a slight bias for T5 inputs; (2) each layer houses a unique ensemble of downstream neurons while sharing a core circuit motif composed of T4/T5, a bilayer LPi cell, and output VPNs; (3) the T4 and T5 axon terminals receive substantial inputs that could refine the local motion direction tuning; (4) new circuit elements

Figure 4. Connectivity of the bilayer lobula plate-intrinsic (LPi) cells

A representative cell of each neuron type is shown in the left panel. Presynaptic sites are indicated with yellow dots, and postsynaptic sites are shown with gray dots. These neurons primarily integrate inputs in one layer and supply outputs to the adjacent layer. Only the LPi3-4 cell is completely reconstructed, while the other cells are only partially reconstructed since single neurons cover larger lobula plate areas than the imaged data volume. A candidate light microscopy match for LPi1-2 (Figure S2) suggests the possibility that the LPi1-2 reconstructions (and perhaps also the similar LPi1-2 fragments) may be parts of one or a few large cells. In the right two panels, the ratios of the input and output synapses are shown for each indicated cell type. These data are based on a single selected branch for each cell type for which the presynaptic and postsynaptic connected neurons were identified wherever possible. Cell types occupying less than 2% of the total input or output synapses are not shown and are included as “other.” Several tangential elements that have synapses with the LPi cells were only partially reconstructed due to the restricted data volume. These fragments of considerable size are grouped as “unidentified LPis and LPTCs.” Data summary is based on Data S3.



(legend on next page)

combine motion signals for different directions, including the Y11 and Y12 cells; and (5) many neurons that convey motion signals from the lobula plate to the lobula, implicating lobula circuitry with a more significant role in motion processing.

We found that all lobula plate neurons that are strongly connected to T4 and T5 axon terminals integrate these inputs in the same layers (Figure 2B). We find a modest but consistent asymmetry, where on average, neurons receive ~20% more synapses from T5 than T4. This may indicate that T5's OFF signals are weighted more heavily than T4's ON signal. Future studies examining the entire lobula plate will be needed to explore broader patterns of T4/T5 connectivity, such as different local biases in different parts of the field of view or for different target neuron types. Nevertheless, we do not find any output neurons that are purely T4 or T5 selective. This is a significant finding that implies, at least for the motion pathway, that the ON/OFF separation is an internal feature. At the output stages of the pathway, ON- and OFF-motion signals are combined onto all prominent lobula plate targets.

Most of the identified LPTCs receive T4/T5 inputs in single layers; however, several VS cells (Figure 3), three columnar VPNs (LLPC1, LLPC1, and LLPC2), and some optic-lobe-intrinsic neurons (e.g., LPi34-12) receive T4/T5 inputs in multiple layers (Figures 2A, 5, and 6). These connectivity patterns suggest that most LPTCs receive large-field motion information from T4/T5 representing the preferred direction of one of the four layers, whereas small-field neurons may integrate signals from multiple layers and as a population could transmit more complex motion information to their downstream neurons. The best-explored example of this is LLPC2, whose looming sensitivity was attributed to T4/T5 and bilayer LPi inputs in all four layers,^{3,4} a hypothesis that this study has substantively confirmed.

Bilayer LPi cells

The four bilayer LPi cells have a common distribution of synapses, with T4/T5 inputs in one layer and output synapses in a neighboring layer, where they presumably inhibit most or all of the neurons that also receive excitatory T4/T5 inputs in that layer (Figures 2A, 4, and 7A), implementing motion opponency.⁴⁰ Although these cell types likely serve similar functions in motion processing, there are also clear anatomical differences. The cell bodies of LPi1-2, LPi2-1, and LPi4-3 are in the lobula plate cortex, whereas LPi3-4s are in the medulla cortex^{15,16,40} and, therefore, likely derive from different precursor cells. EM and LM data suggest substantial size differences among the bilayer LPis, with LPi3-4 likely being the smallest arborization and individual LPi1-2 cells arborizing across much of the lobula plate (Figure S2A). Since the spatial coverage of individual LPi neurons differs

between the types, the spatial integration of opponent signals may differ between layers for reasons that are unclear. All 4 bilayer LPi types provide inputs to both large- and small-field neurons (e.g., LPi1-2 is upstream of H2 and also LPC1; Figures 4, 5A, and 5R), so there is no simple relationship between the apparent receptive field size of the different LPi neurons and the receptive field sizes of their major targets. These differences raise questions about the evolution of the bilayer LPi cells. Are these LPis derived from a shared ancestral cell type, for example, via duplication, that later substantially diverged in some of their anatomical properties, or did the antiparallel inhibition mediated by the bilayer LPis evolve independently in different layers?

Y cells encoding oblique motion directions

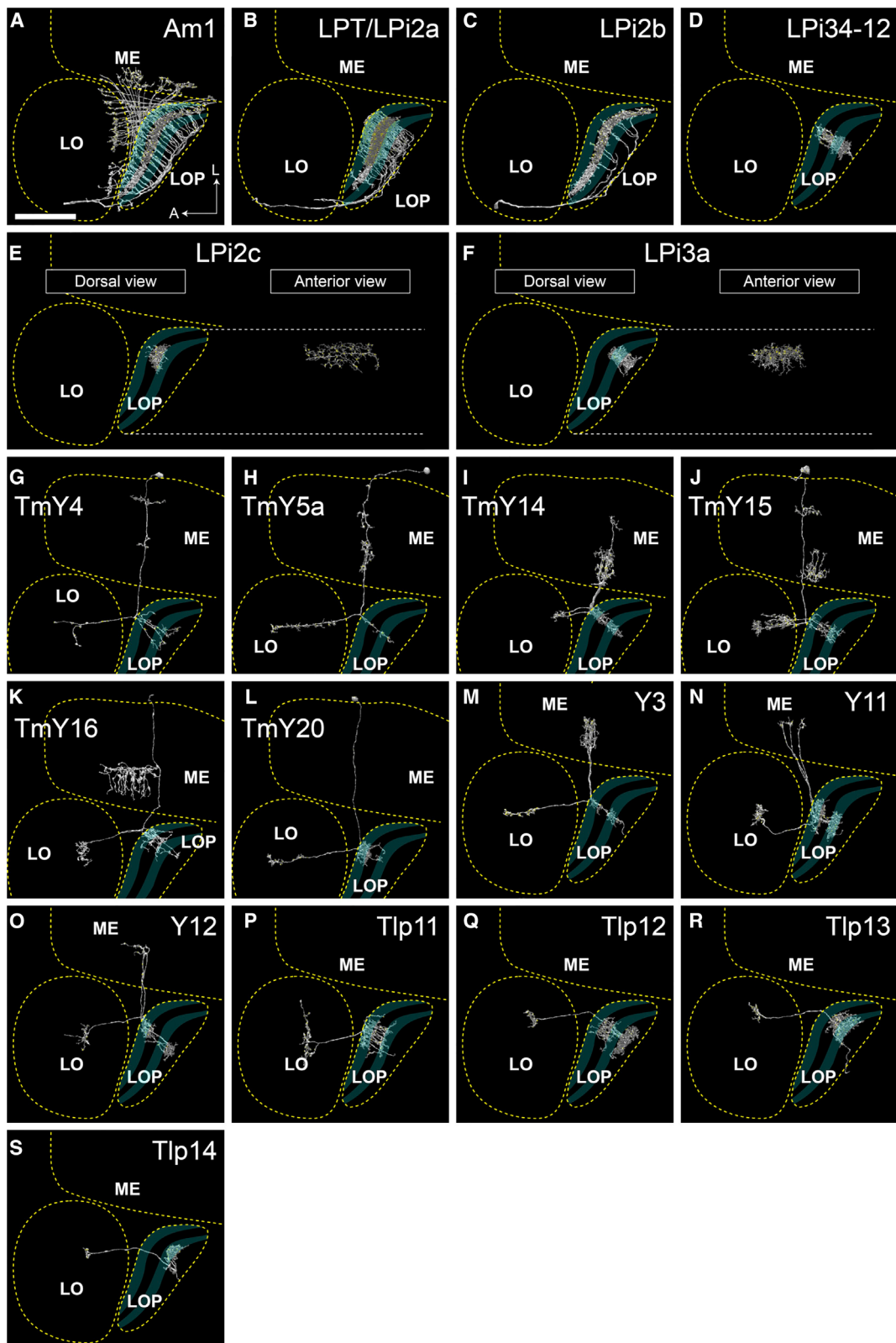
We discovered that Y11 and Y12 integrate motion information in two layers and thus likely synthesize a preferred tuning for a new, oblique direction of motion (Figures 2A and 7B). These neurons effectively fill two gaps between the four directions represented by T4/T5 subtypes. Y11 and Y12 are also major sources of inputs to T4 and T5 neurons (Data S1), suggesting that they may alter the local directional preference of T4 and T5. Clarifying the role of these Y cells will require establishing whether they are excitatory or inhibitory (inhibition via glutamate is a strong possibility, as T4/T5 axons express GluCl α , a glutamate-gated chloride channel,⁶⁶ yet are not strong targets of the bilayer LPi neurons; Figure 4; Data S1). These recurrent connections could provide a possible mechanistic explanation for the functionally identified subtypes of T4/T5;³⁶ however, this recent study found subtypes in layers 1 and 2, whereas Y11 and Y12 collect outputs and provide inputs to layers 1, 3, and 4. Both neurons combine a vertical motion signal with front-to-back motion, but we did not find complementary neurons for the oblique motion directions integrating Lop2/back-to-front motion. Beyond this role in the lobula plate, these Y cells are presynaptic in the lobula and medulla (Figures 6N, 6O, and 7D). Identifying the targets of Y11 and Y12 will be an important goal of future connectomes.

Expanding the horizontal motion detection circuit with new cell types

Our detailed analysis suggests that several new connections should be added to the existing models of binocular integration of rotational optic flow derived from work on blowflies.³⁸ The Am1 cell, which receives inputs from ipsilateral T4b/T5b and contralateral H1, likely combines optic flow across both eyes. H1 expresses a marker for glutamatergic neurons.⁵² In *Drosophila*, glutamate could function as either excitatory or inhibitory, whereas in the blowfly, H1 seems to provide excitatory

Figure 5. Lobula plate visual projection neurons (VPNs) that integrate T4 and T5 inputs

The neurons are seen from the dorsal direction (horizontal projection), the approximate neuropil boundaries are outlined, and the lobula plate layers are indicated. Only neurons mentioned in other figures or in the main text are shown here. (A) LPC1, (B) LPC2, (C) LLPC1, (D) LLPC2, (E) LLPC3, (F) LPi1, (G) LPi2, (H) LPi1b, (I) LPi2-1, (J) LPi3-1, (K) LPi3-2, (L) LPi3-3, (M) LPi3-4, (N) LPi4-1, (O) LPi4-2, (P) DCH, (Q) H1, and (R) H2. Some neurons are not fully reconstructed, especially the cell body fibers and the main axons projecting to the central brain. Lobula plate-lobula columnar (LLPC) cells have cell bodies in the cell body rind between the optic lobe and central brain and dendritic arbors in the lobula that extend into the lobula plate^{43,45} and project to the central brain from the lobula. Lobula plate columnar (LPC) and lobula-lobula plate columnar (LLPC) cells have cell bodies in the cell body rind of the lobula plate^{43,45,46,48,49} and project axons along a path posterior to the lobula plate to glomeruli in the posterior lateral protocerebrum. Both LPC and LLPC send a branch into the lobula plate that, in the case of LLPC cells, further extends into the lobula. HS and VS cells are omitted from this figure (see Figure 3). In (R), the branching pattern and synapse distribution are shown in the inset. Presynapses and postsynapses are shown in magenta and gray, respectively. In (A), A, anterior; L, lateral. Scale bars, 30 μ m (A–S) and 20 μ m (R, inset).



(legend on next page)

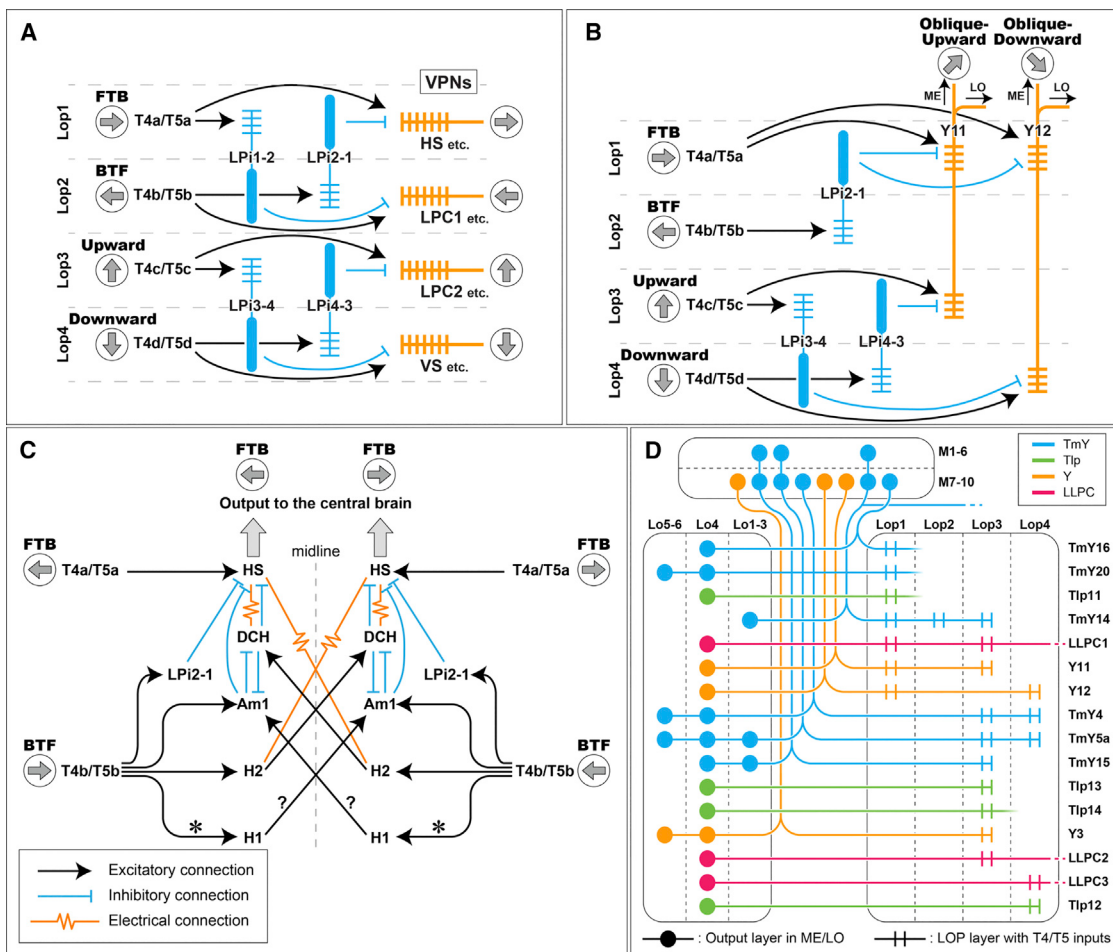


Figure 7. Summary of the motion pathway circuitry revealed by the lobula plate reconstruction

(A) The primary connections between the T4/T5 cells, bilayer LPI cells, and output VPNs. FTB, front-to-back; BTF, back-to-front. The LPI cells, indicated in blue, are likely all inhibitory cells.⁴⁰ Each layer has VPN outputs that are predicted (or known for the few supported by functional studies) to encode motion with the same directional selectivity as the T4/T5 subtypes in that layer. Some VPNs, like the VS cells of Figure 3, integrate inputs from multiple T4/T5 subtypes in different layers. (B) The Y11 and Y12 cells and their lobula plate inputs. The two Y cell types receive excitatory inputs from T4 and T5 in two layers and (putative) inhibitory inputs from T4 and T5 neurons in the other layers, via bilayer LPI cells. By integrating these inputs, it is expected that these neurons become most sensitive to the direction of overlapping sensitivity of their inputs, and thus, Y11's preferred direction would be oblique-upward motion, and Y12 would prefer oblique-downward motion. (C) The bilateral circuitry comprised horizontal-motion-sensitive neurons, including H1, H2, DCH, and Am1 cells, integrating motion from both eyes. Connections within the optic lobe are based on the observation of this dataset, whereas contralateral projections and synaptic contacts in the central brain are also based on previous studies and datasets, including Farrow et al.^{38,51} and Scheffer et al.⁴⁸ Connections from T4b/T5b to H1, indicated with asterisks (*), are shown in Figure S1. H1 is considered to be a glutamatergic cell,⁵² and it is not known whether the signal from H1 is excitatory or inhibitory. Since electrical synapses cannot be directly observed in the FIB-SEM dataset, the indicated connections are based on prior work and the physical proximity of the axons of these cells in this dataset. The diagrams do not exhaustively list the inputs and outputs of the shown neurons. (D) Neurons relaying T4/T5 outputs to the lobula. The paired parallel lines indicate T4/T5 inputs in the lobula plate, whereas the dots represent the locations of the output (presynaptic) terminals in the lobula and the medulla. Input (postsynaptic) terminals in the lobula and the medulla, as well as terminals not connected to T4/T5 in the lobula plate, are omitted. The central brain projections of TmY14 and the LLPC cells are shown as broken lines.

signals.³⁹ T4b and T5b detect back-to-front movement and, via (putative) inhibitory LPI2-1 cells, suppress the activity of Lop1 neurons, including HS cells (Figure 7C). Am1 may represent

two more pathways for suppressing the activity of HS cells in response to back-to-front motion inputs directly and through DCH, which is also electrically coupled with HS in *Calliphora*.³⁸

Figure 6. Optic lobe-intrinsic neurons that integrate T4 and T5 inputs

The neurons are seen from the dorsal direction (horizontal projection), the approximate neuropil boundaries are outlined, and the lobula plate layers are indicated. Only neurons mentioned in other figures or in the main text are shown here. (A) Am1, (B) LPT/LPI2a, (C) LPI2b, (D) LPI34-12, (E) LPI2c, (F) LPI3a, (G) TmY4, (H) TmY5a, (I) TmY14, (J) TmY15, (K) TmY16, (L) TmY20, (M) Y3, (N) Y11, (O) Y12, (P) Tlp11, (Q) Tlp12, (R) Tlp13, and (S) Tlp14. Some of the neurons are not fully reconstructed, especially the cell body fibers. We confirmed the general cell shapes of all newly identified cell types shown in this figure (with the exception of the comparatively small LPI2c and LPI3a fragments) by comparison to light microscopy images (Figures S2 and S3). Based on these matches, LPT/LPI2a may be a type of VPN with a central brain projection. Presynapses and postsynapses are shown in magenta and gray, respectively. Scale bars, 30 μm.

Both excitatory and inhibitory motion signals are integrated at different scales: the scale of bilayer LPi neurons and the CH neurons, and over the entire field of view by combining contralateral optic flow transmitted by H1 and H2 (Figure 7C). These proposals also highlight a limitation of connectomic studies for predicting the selectivity of these neurons. We have mainly described VPN selectivity as a function of their feedforward T4/T5 input; however, the resultant selectivity of any neuron to visual motion patterns depends on feedback connections from other neurons in the lobula plate, as well as inputs received in the central brain.^{38,39} Connectomic studies establish chemical synapses but do not generally reveal electrical synapses (gap junctions). Gap junction predictions from light microscopic analyses⁶⁷ often require further confirmation, and determining how electrical connections shape the functional logic of these circuits will require detailed neurophysiological studies.

Multiple neuron types convey T4/T5 signals to specific lobula layers

We found that T4/T5 are connected to several neuron types that likely relay these signals within the optic lobe. For example, TmY20 cells (Figure 6L) receive the largest share of T4a/T5a output synapses (Figure 2A). Although the standard circuit models of the motion pathways, which comprise T4/T5, LPTCs, and bilayer interneurons (Figure 7A), have remained compact, evidence for additional, strong pathways reveal that motion signals are integrated into a broader set of downstream circuits than previously suggested. Many T4/T5 downstream cells, including Tlp, LLPC, and TmY neurons (Figures 2, 5, and 6), project to the lobula, where they mainly target layer Lo4 (Figure 7D). The circuits of the lobula, outside of T5 inputs in Lo1, have been scarcely examined. Motion signals from the lobula plate should significantly contribute to visual processing in the lobula, and many VPNs could inherit motion signals from the lobula plate without any input sites there. The complete description of these pathways and their extended circuits will require an EM dataset that covers nearly the entire brain.

Toward the complete reconstruction of sensory-to-motor pathways

The connectivity profile of T4/T5 neurons in the lobula plate details a large missing part of the motion pathways, the link between motion detection and output neurons of the optic lobe. With this stage finally reconstructed, the motion pathway from the photoreceptor cells to the central brain can now be traced neuron by neuron by combining results across EM reconstructions.^{15,20–22,24,68} Many of the VPNs we reconstructed are also identified in the hemibrain dataset⁴⁸ that contains much of the central brain, enabling the comprehensive identification of downstream circuits to extend the described pathways further. The strength of our study—the detailed analysis of a central region of the lobula plate—is also a limitation. The diversity of cells downstream of the lobula plate is certainly larger than we described here, and we hope that future studies in larger EM volumes^{59,69} will cover the entire lobula plate. Many of our new discoveries suggest a more integrative picture of optic lobe processing, where the lobula plate is no longer seen as the sole substrate for motion processing but rather is understood to organize ON and OFF directionally selective signals

for a variety of as-yet-unexplored roles in visually guided behaviors.

STAR★METHODS

Detailed methods are provided in the online version of this paper and include the following:

- KEY RESOURCES TABLE
- RESOURCE AVAILABILITY
 - Lead contact
 - Materials availability
 - Data and code availability
- EXPERIMENTAL MODEL AND SUBJECT DETAILS
- METHOD DETAILS
 - The EM dataset
 - Reconstruction of the neurons and the neuron nomenclature
 - Light microscopy (LM) and LM/EM comparison
- QUANTIFICATION AND STATISTICAL ANALYSIS

SUPPLEMENTAL INFORMATION

Supplemental information can be found online at <https://doi.org/10.1016/j.cub.2022.06.061>.

ACKNOWLEDGMENTS

The authors thank members of the FlyEM Project Team at Janelia Research Campus for the sample preparation, image acquisition, image processing, and proofreading of the neurons and synapses and the FlyLight Project Team for light microscopy images. We especially thank Stuart Berg, Lowell Umayam, and William Katz of the FlyEM Team for data management and preparing neuPrint/Neuroglancer data and Gerry Rubin and the members of the FlyEM steering committee for supporting this project. We also thank the members of the Reiser lab for the fruitful discussions and advice on the analysis. This project was supported by the Howard Hughes Medical Institute.

AUTHOR CONTRIBUTIONS

Conceptualization, K.S., A.N., and M.B.R.; formal analysis, K.S.; funding acquisition, S.M.P. and M.B.R.; investigation, K.S. and A.N.; methodology, K.S.; supervision, I.A.M., S.M.P., and M.B.R.; visualization, K.S. and A.N.; writing – original draft, K.S., A.N., and M.B.R.; writing – review & editing, K.S., A.N., and M.B.R.

DECLARATION OF INTERESTS

The authors declare no competing interests.

Received: December 20, 2021

Revised: May 17, 2022

Accepted: June 20, 2022

Published: July 14, 2022

REFERENCES

1. Muijres, F.T., Elzinga, M.J., Melis, J.M., and Dickinson, M.H. (2014). Flies evade looming targets by executing rapid visually directed banked turns. *Science* 344, 172–177. <https://doi.org/10.1126/science.1248955>.
2. Borst, A., Haag, J., and Reiff, D.F. (2010). Fly motion vision. *Annu. Rev. Neurosci.* 33, 49–70. <https://doi.org/10.1146/annurev-neuro-060909-153155>.
3. Ache, J.M., Polksky, J., Alghailani, S., Parekh, R., Breads, P., Peek, M.Y., Bock, D.D., von Reyn, C.R., and Card, G.M. (2019). Neural basis for

- looming size and velocity encoding in the *Drosophila* giant fiber escape pathway. *Curr. Biol.* 29, 1073–1081.e4. <https://doi.org/10.1016/j.cub.2019.01.079>.
4. Klapoetke, N.C., Nern, A., Peek, M.Y., Rogers, E.M., Breads, P., Rubin, G.M., Reiser, M.B., and Card, G.M. (2017). Ultra-selective looming detection from radial motion opponency. *Nature* 551, 237–241. <https://doi.org/10.1038/nature24626>.
 5. Morimoto, M.M., Nern, A., Zhao, A., Rogers, E.M., Wong, A.M., Isaacson, M.D., Bock, D.D., Rubin, G.M., and Reiser, M.B. (2020). Spatial readout of visual looming in the central brain of *Drosophila*. *eLife* 9, e57685, <https://doi.org/10.7554/eLife.57685>.
 6. Song, B.M., and Lee, C.H. (2018). Toward a mechanistic understanding of color vision in insects. *Front. Neural Circuits* 12, 16. <https://doi.org/10.3389/fncir.2018.00016>.
 7. Schnaitmann, C., Haikala, V., Abraham, E., Oberhauser, V., Thestrup, T., Griesbeck, O., and Reiff, D.F. (2018). Color processing in the early visual system of *Drosophila*. *Cell* 172, 318–330.e18. <https://doi.org/10.1016/j.cell.2017.12.018>.
 8. Behnia, R., Clark, D.A., Carter, A.G., Clandinin, T.R., and Desplan, C. (2014). Processing properties of ON and OFF pathways for *Drosophila* motion detection. *Nature* 512, 427–430. <https://doi.org/10.1038/nature13427>.
 9. Maisak, M.S., Haag, J., Ammer, G., Serbe, E., Meier, M., Leonhardt, A., Schilling, T., Bahl, A., Rubin, G.M., Nern, A., et al. (2013). A directional tuning map of *Drosophila* elementary motion detectors. *Nature* 500, 212–216. <https://doi.org/10.1038/nature12320>.
 10. Brand, A.H., and Perrimon, N. (1993). Targeted gene expression as a means of altering cell fates and generating dominant phenotypes. *Development* 118, 401–415.
 11. Duffy, J.B. (2002). GAL4 system in *Drosophila*: a fly geneticist's Swiss army knife. *Genesis* 34, 1–15. <https://doi.org/10.1002/gen.10150>.
 12. Jenett, A., Rubin, G.M., Ngo, T.T., Shepherd, D., Murphy, C., Dionne, H., Pfeiffer, B.D., Cavallaro, A., Hall, D., Jeter, J., et al. (2012). A GAL4-driver line resource for *Drosophila* neurobiology. *Cell Rep.* 2, 991–1001. <https://doi.org/10.1016/j.celrep.2012.09.011>.
 13. Simpson, J.H. (2016). Rationally subdividing the fly nervous system with versatile expression reagents. *J. Neurogenet.* 30, 185–194. <https://doi.org/10.1080/01677063.2016.1248761>.
 14. Borst, A. (2009). *Drosophila*'s view on insect vision. *Curr. Biol.* 19, R36–R47. <https://doi.org/10.1016/j.cub.2008.11.001>.
 15. Shinomiya, K., Huang, G., Lu, Z., Parag, T., Xu, C.S., Aniceto, R., Ansari, N., Cheatham, N., Lauchie, S., Neace, E., et al. (2019). Comparisons between the ON- and OFF-edge motion pathways in the *Drosophila* brain. *eLife* 8, e40025, <https://doi.org/10.7554/eLife.40025>.
 16. Fischbach, K.-F., and Dittrich, A.P.M. (1989). The optic lobe of *Drosophila melanogaster*. I. A Golgi analysis of wild-type structure. *Cell Tissue Res.* 258, 441–475.
 17. Strausfeld, N.J. (1976). *Atlas of An Insect Brain* (Springer-Verlag).
 18. Nern, A., Pfeiffer, B.D., and Rubin, G.M. (2015). Optimized tools for multi-color stochastic labeling reveal diverse stereotyped cell arrangements in the fly visual system. *Proc. Natl. Acad. Sci. USA* 112, E2967–E2976. <https://doi.org/10.1073/pnas.1506763112>.
 19. Tirian, L., and Dickson, B. (2017). The VT GAL4, LexA, and split-GAL4 driver line collections for targeted expression in the *Drosophila* nervous system. Preprint at bioRxiv. <https://doi.org/10.1101/198648>.
 20. Rivera-Alba, M., Vitaladevuni, S.N., Mishchenko, Y., Lu, Z., Takemura, S.Y., Scheffer, L., Meinertzhagen, I.A., Chklovskii, D.B., and de Polavieja, G.G. (2011). Wiring economy and volume exclusion determine neuronal placement in the *Drosophila* brain. *Curr. Biol.* 21, 2000–2005. <https://doi.org/10.1016/j.cub.2011.10.022>.
 21. Takemura, S.Y., Lu, Z., and Meinertzhagen, I.A. (2008). Synaptic circuits of the *Drosophila* optic lobe: the input terminals to the medulla. *J. Comp. Neurol.* 509, 493–513. <https://doi.org/10.1002/cne.21757>.
 22. Takemura, S.Y., Bharioke, A., Lu, Z., Nern, A., Vitaladevuni, S., Rivlin, P.K., Katz, W.T., Olbris, D.J., Plaza, S.M., Winston, P., et al. (2013). A visual motion detection circuit suggested by *Drosophila* connectomics. *Nature* 500, 175–181. <https://doi.org/10.1038/nature12450>.
 23. Takemura, S.Y., Nern, A., Chklovskii, D.B., Scheffer, L.K., Rubin, G.M., and Meinertzhagen, I.A. (2017). The comprehensive connectome of a neural substrate for 'ON' motion detection in *Drosophila*. *eLife* 6, e24394, <https://doi.org/10.7554/eLife.24394>.
 24. Shinomiya, K., Karuppudurai, T., Lin, T.Y., Lu, Z., Lee, C.H., and Meinertzhagen, I.A. (2014). Candidate neural substrates for off-edge motion detection in *Drosophila*. *Curr. Biol.* 24, 1062–1070. <https://doi.org/10.1016/j.cub.2014.03.051>.
 25. Strother, J.A., Wu, S.T., Wong, A.M., Nern, A., Rogers, E.M., Le, J.Q., Rubin, G.M., and Reiser, M.B. (2017). The emergence of directional selectivity in the visual motion pathway of *Drosophila*. *Neuron* 94, 168–182.e10. <https://doi.org/10.1016/j.neuron.2017.03.010>.
 26. Serbe, E., Meier, M., Leonhardt, A., and Borst, A. (2016). Comprehensive characterization of the major presynaptic elements to the *Drosophila* OFF motion detector. *Neuron* 89, 829–841. <https://doi.org/10.1016/j.neuron.2016.01.006>.
 27. Strausfeld, N.J. (2021). The lobula plate is exclusive to insects. *Arthropod Struct. Dev.* 61, 101031, <https://doi.org/10.1016/j.asd.2021.101031>.
 28. Hausen, K., and Egelhaaf, M. (1989). Neural mechanisms of visual course control in insects. In *Facets of Vision*, D.G. Stavenga, and R.C. Hardie, eds. (Springer), pp. 391–424.
 29. Hausen, K. (1984). The lobula-complex of the fly: structure, function and significance in visual behaviour. In *Photoreception and Vision in Invertebrates*, M.A. Ali, ed. (Springer), pp. 523–559. https://doi.org/10.1007/978-1-4613-2743-1_15.
 30. Eckert, H. (1980). Functional properties of the H1-neurone in the third optic ganglion of the blowfly, *Phaenicia*. *J. Comp. Physiol.* 135, 29–39. <https://doi.org/10.1007/BF00660179>.
 31. Hausen, K. (1976). Functional characterization and anatomical identification of motion sensitive neurons in the lobula plate of the blowfly *Calliphora erythrocephala*. *Z. Naturforsch. C* 31, 629–634.
 32. Krapp, H.G., and Hengstenberg, R. (1996). Estimation of self-motion by optic flow processing in single visual interneurons. *Nature* 384, 463–466. <https://doi.org/10.1038/384463a0>.
 33. Scott, E.K., Raabe, T., and Luo, L. (2002). Structure of the vertical and horizontal system neurons of the lobula plate in *Drosophila*. *J. Comp. Neurol.* 454, 470–481. <https://doi.org/10.1002/cne.10467>.
 34. Joesch, M., Plett, J., Borst, A., and Reiff, D.F. (2008). Response properties of motion-sensitive visual interneurons in the lobula plate of *Drosophila melanogaster*. *Curr. Biol.* 18, 368–374. <https://doi.org/10.1016/j.cub.2008.02.022>.
 35. Schnell, B., Joesch, M., Forstner, F., Raghu, S.V., Otsuna, H., Ito, K., Borst, A., and Reiff, D.F. (2010). Processing of horizontal optic flow in three visual interneurons of the *Drosophila* brain. *J. Neurophysiol.* 103, 1646–1657. <https://doi.org/10.1152/jn.00950.2009>.
 36. Henning, M., Ramos-Trasloseros, G., Gür, B., and Silies, M. (2022). Populations of local direction-selective cells encode global motion patterns generated by self-motion. *Sci. Adv.* 8, eabi7112. <https://doi.org/10.1126/sciadv.abi7112>.
 37. Boergens, K.M., Kapfer, C., Helmstaedter, M., Denk, W., and Borst, A. (2018). Full reconstruction of large lobula plate tangential cells in *Drosophila* from a 3D EM dataset. *PLoS One* 13, e0207828, <https://doi.org/10.1371/journal.pone.0207828>.
 38. Farrow, K., Haag, J., and Borst, A. (2006). Nonlinear, binocular interactions underlying flow field selectivity of a motion-sensitive neuron. *Nat. Neurosci.* 9, 1312–1320. <https://doi.org/10.1038/nn1769>.
 39. Haag, J., and Borst, A. (2001). Recurrent network interactions underlying flow-field selectivity of visual interneurons. *J. Neurosci.* 21, 5685–5692.

40. Mauss, A.S., Pankova, K., Arenz, A., Nern, A., Rubin, G.M., and Borst, A. (2015). Neural circuit to integrate opposing motions in the visual field. *Cell* 162, 351–362. <https://doi.org/10.1016/j.cell.2015.06.035>.
41. Raghu, S.V., and Borst, A. (2011). Candidate glutamatergic neurons in the visual system of *Drosophila*. *PLoS One* 6, e19472, <https://doi.org/10.1371/journal.pone.0019472>.
42. Mauss, A.S., Meier, M., Serbe, E., and Borst, A. (2014). Optogenetic and pharmacologic dissection of feedforward inhibition in *Drosophila* motion vision. *J. Neurosci.* 34, 2254–2263. <https://doi.org/10.1523/JNEUROSCI.3938-13.2014>.
43. Wu, M., Nern, A., Williamson, W.R., Morimoto, M.M., Reiser, M.B., Card, G.M., and Rubin, G.M. (2016). Visual projection neurons in the *Drosophila* lobula link feature detection to distinct behavioral programs. *eLife* 5, e21022, <https://doi.org/10.7554/eLife.21022>.
44. Gilbert, C., and Strausfeld, N.J. (1991). The functional organization of male-specific visual neurons in flies. *J. Comp. Physiol. A* 169, 395–411. <https://doi.org/10.1007/BF00197653>.
45. Panser, K., Tirian, L., Schulze, F., Villalba, S., Jefferis, G.S.X.E., Bühler, K., and Straw, A.D. (2016). Automatic segmentation of *Drosophila* neural compartments using GAL4 expression data reveals novel visual pathways. *Curr. Biol.* 26, 1943–1954. <https://doi.org/10.1016/j.cub.2016.05.052>.
46. Davis, F.P., Nern, A., Picard, S., Reiser, M.B., Rubin, G.M., Eddy, S.R., and Henry, G.L. (2020). A genetic, genomic, and computational resource for exploring neural circuit function. *eLife* 9, e50901, <https://doi.org/10.7554/eLife.50901>.
47. Strausfeld, N.J., and Okamura, J.Y. (2007). Visual system of calliphorid flies: organization of optic glomeruli and their lobula complex efferents. *J. Comp. Neurol.* 500, 166–188. <https://doi.org/10.1002/cne.21196>.
48. Scheffer, L.K., Xu, C.S., Januszewski, M., Lu, Z., Takemura, S.Y., Hayworth, K.J., Huang, G.B., Shinomiya, K., Maitlin-Shepard, J., Berg, S., et al. (2020). A connectome and analysis of the adult *Drosophila* central brain. *eLife* 9, e57443, <https://doi.org/10.7554/eLife.57443>.
49. Isaacson, M.D. (2019). Using new tools to study the neural mechanisms of sensation: auditory processing in locusts and translational motion vision in flies. PhD thesis (University of Cambridge).
50. Shinomiya, K., Horne, J.A., McLin, S., Wiederman, M., Nern, A., Plaza, S.M., and Meinertzhagen, I.A. (2019). The organization of the second optic chiasm of the *drosophila* optic lobe. *Front. Neural Circuits* 13, 65. <https://doi.org/10.3389/fncir.2019.00065>.
51. Farrow, K., Haag, J., and Borst, A. (2003). Input organization of multifunctional motion-sensitive neurons in the blowfly. *J. Neurosci.* 23, 9805–9811.
52. Wei, H., Kyung, H.Y., Kim, P.J., and Desplan, C. (2020). The diversity of lobula plate tangential cells (LPTCs) in the *Drosophila* motion vision system. *J. Comp. Physiol. A Neuroethol. Sens. Neural Behav. Physiol.* 206, 139–148. <https://doi.org/10.1007/s00359-019-01380-y>.
53. Haag, J., Vermeulen, A., and Borst, A. (1999). The intrinsic electrophysiological characteristics of fly lobula plate tangential cells: III. Visual response properties. *J. Comput. Neurosci.* 7, 213–234. <https://doi.org/10.1023/a:1008950515719>.
54. Hengstenberg, R. (1982). Common visual response properties of giant vertical cells in the lobula plate of the blowfly *Calliphora*. *J. Comp. Physiol.* 149, 179–193. <https://doi.org/10.1007/BF00619212>.
55. Pierantoni, R. (1976). A look into the cock-pit of the fly. The architecture of the lobular plate. *Cell Tissue Res.* 171, 101–122. <https://doi.org/10.1007/BF00219703>.
56. Hengstenberg, R., Hausen, K., and Hengstenberg, B. (1982). The number and structure of giant vertical cells (VS) in the lobula plate of the blowfly *Calliphora erythrocephala*. *J. Comp. Physiol.* 149, 163–177.
57. Kim, A.J., Fenk, L.M., Lyu, C., and Maimon, G. (2017). Quantitative predictions orchestrate visual signaling in *Drosophila*. *Cell* 168, 280–294.e12. <https://doi.org/10.1016/j.cell.2016.12.005>.
58. Barnhart, E.L., Wang, I.E., Wei, H., Desplan, C., and Clandinin, T.R. (2018). Sequential nonlinear filtering of local motion cues by global motion circuits. *Neuron* 100, 229–243.e3. <https://doi.org/10.1016/j.neuron.2018.08.022>.
59. Zheng, Z., Lauritzen, J.S., Perlman, E., Robinson, C.G., Nichols, M., Milkiewicz, D., Torrens, O., Price, J., Fisher, C.B., Sharifi, N., et al. (2018). A complete electron microscopy volume of the brain of adult *Drosophila melanogaster*. *Cell* 174, 730–743.e22. <https://doi.org/10.1016/j.cell.2018.06.019>.
60. Eckert, H., and Dvorak, D.R. (1983). The centrifugal horizontal cells in the lobula plate of the blowfly, *Phaenicia sericata*. *J. Insect Physiol.* 29, 547–560.
61. Gauck, V., Egelhaaf, M., and Borst, A. (1997). Synapse distribution on VCH, an inhibitory, motion-sensitive interneuron in the fly visual system. *J. Comp. Neurol.* 381, 489–499.
62. Meyer, E.P., Matute, C., Streit, P., and Nässel, D.R. (1986). Insect optic lobe neurons identifiable with monoclonal antibodies to GABA. *Histochemistry* 84, 207–216. <https://doi.org/10.1007/BF00495784>.
63. Duistermars, B.J., Care, R.A., and Frye, M.A. (2012). Binocular interactions underlying the classic optomotor responses of flying flies. *Front. Behav. Neurosci.* 6, 6. <https://doi.org/10.3389/fnbeh.2012.00006>.
64. Bishop, C.A., and Bishop, L.G. (1981). Vertical motion detectors and their synaptic relations in the third optic lobe of the fly. *J. Neurobiol.* 12, 281–296. <https://doi.org/10.1002/neu.480120308>.
65. Dvorak, D.R., Bishop, L.G., and Eckert, H.E. (1975). On the identification of movement detectors in the fly optic lobe. *J. Comp. Physiol.* 100, 5–23.
66. Fendt, S., Vieira, R.M., and Borst, A. (2020). Conditional protein tagging methods reveal highly specific subcellular distribution of ion channels in motion-sensing neurons. *eLife* 9, e62953, <https://doi.org/10.7554/eLife.62953>.
67. Ammer, G., Vieira, R.M., Fendt, S., and Borst, A. (2022). Anatomical distribution and functional roles of electrical synapses in *Drosophila*. *Curr. Biol.* 32, 2022–2036.e4. <https://doi.org/10.1016/j.cub.2022.03.040>.
68. Takemura, S.Y., Xu, C.S., Lu, Z., Rivlin, P.K., Parag, T., Olbris, D.J., Plaza, S., Zhao, T., Katz, W.T., Umayam, L., et al. (2015). Synaptic circuits and their variations within different columns in the visual system of *Drosophila*. *Proc. Natl. Acad. Sci. USA* 112, 13711–13716. <https://doi.org/10.1073/pnas.1509820112>.
69. Dorkenwald, S., McKellar, C.E., Macrina, T., Kemnitz, N., Lee, K., Lu, R., Wu, J., Popovych, S., Mitchell, E., Nehorai, B., et al. (2022). FlyWire: online community for whole-brain connectomics. *Nat. Methods* 19, 119–128. <https://doi.org/10.1038/s41592-021-01330-0>.
70. Feng, L., Zhao, T., and Kim, J. (2015). neuTube 1.0: a new design for efficient neuron reconstruction software based on the SWC format. *ENEURO* 2, 0049–0014.2014.
71. Clements, J., Dolafi, T., Umayam, L., Neubarth, N.L., Berg, S., Scheffer, L.K., and Plaza, S.M. (2020). neuPrint: analysis tools for EM connectomics. Preprint at bioRxiv. <https://doi.org/10.1101/2020.01.16.909465>.
72. Otsuna, H., and Ito, K. (2006). Systematic analysis of the visual projection neurons of *Drosophila melanogaster*. I. Lobula-specific pathways. *J. Comp. Neurol.* 497, 928–958. <https://doi.org/10.1002/cne.21015>.

STAR★METHODS

KEY RESOURCES TABLE

REAGENT or RESOURCE	SOURCE	IDENTIFIER
Experimental models: Organisms/strains		
<i>D. melanogaster</i> : <i>w</i> ¹¹¹⁸	Janelia Research Campus	N/A
<i>D. melanogaster</i> : Canton S	Janelia Research Campus	N/A
<i>D. melanogaster</i> : MCFO-1	Nern et al., 2015 ¹⁸	RRID: BDSC_64085
<i>D. melanogaster</i> : MCFO-7	Nern et al., 2015 ¹⁸	RRID: BDSC_64091
<i>D. melanogaster</i> : R20F11-GAL4	Jenett et al., 2012 ¹²	RRID: BDSC_49852
<i>D. melanogaster</i> : R15D05-Gal4	Jenett et al., 2012 ¹²	RRID: BDSC_48686
<i>D. melanogaster</i> : R42B05-GAL4	Jenett et al., 2012 ¹²	RRID: BDSC_41246
<i>D. melanogaster</i> : OL-KD (29C07-KDGeneswitch-4) in attP40; R57C10-GAL4 in attP2 tubP-KDRT>GAL80- 6-KDRT> in VK00027	Nern et al., 2015 ¹⁸	N/A
<i>D. melanogaster</i> : VT048842-GAL4	Tirian and Dickson, 2017 ¹⁹	N/A
<i>D. melanogaster</i> : R11D02-GAL4	Jenett et al., 2012 ¹²	RRID: BDSC_48452
<i>D. melanogaster</i> : R10E08-GAL4	Jenett et al., 2012 ¹²	RRID: BDSC_47842
<i>D. melanogaster</i> : R87B02-GAL4	Jenett et al., 2012 ¹²	RRID: BDSC_41316
<i>D. melanogaster</i> : VT016795-GAL4	Tirian and Dickson, 2017 ¹⁹	N/A
<i>D. melanogaster</i> : VT016279-GAL4	Tirian and Dickson, 2017 ¹⁹	N/A
Software and algorithms		
NeuTu	Feng et al., 2015 ⁷⁰	https://github.com/janelia-flyem/NeuTu
VVD viewer	T. Kawase and K. Rokicki	https://github.com/takashi310/VVD_Visualization
Cytoscape	https://cytoscape.org/	https://cytoscape.org/

RESOURCE AVAILABILITY

Lead contact

Further information and requests for resources and reagents should be directed to and will be fulfilled by the lead contact, Kazunori Shinomiya (kshinomiya@flatironinstitute.org).

Materials availability

This study did not generate new unique reagents.

Data and code availability

The connectivity data as well as 3D data of the reconstructed neurons are available at <https://neuprint.janelia.org/> through neuPrint, an online tool for accessing and analyzing connectome data.⁷¹ Optic lobe neurons including the lobula plate neurons and their connectivity profiles can be searched by selecting “fib19” in the pulldown menu. Grayscale data of the image volume can be browsed via Neuroglancer (<https://github.com/google/neuroglancer>) through the neuPrint interface. The seed T4 and T5 are identified by “rep” (representative) in the instance names (as in the supplemental tables). Names/annotations that are only listed as instances but not type information are more preliminary. The database contains skeletons and synapse information (and, in some cases, type annotations) beyond what is in this work and the two previous papers^{15,50} on this dataset. These data should be treated with appropriate caution as they are not proofread.

Original light microscopy images are available for download online at http://gen1mcfo.janelia.org/cgi-bin/view_gen1mcfo_imager.cgi?slidecode=slidecode with the appropriate slide code from Table S1 replacing *slidecode*.

EXPERIMENTAL MODEL AND SUBJECT DETAILS

The tissue for the EM sample was obtained from the right optic lobe of a 6-day post-eclosion female fruit fly, *Drosophila melanogaster*, a cross between homozygous *w*¹¹¹⁸ and CS wild type.

METHOD DETAILS

The EM dataset

All of the results presented in this manuscript were based on the same optic lobe FIB-SEM data volume that was used in two previous studies.^{15,50} The tissue was imaged with FIB-SEM with an isotropic voxel resolution ($x = y = z = 8 \text{ nm}$). The size of the image stack is $19,162 \times 10,657 \times 22,543$ pixels, equivalent to $153 \mu\text{m} \times 85 \mu\text{m} \times 180 \mu\text{m}$ of the brain. For more information, see results section EM reconstruction of synaptic partners of T4 and T5 cells in the lobula plate and our previous publication.¹⁵

Reconstruction of the neurons and the neuron nomenclature

Neuronal profiles were automatically segmented, and synaptic motifs (presynaptic T-bars and postsynaptic densities) were predicted throughout the volume as described previously.¹⁵ Predicted synapses reliably reveal connectivity of most neurons and polarity of most synaptic connections,¹⁵ while they include some false-positive and false-negative synapses. For the main connectivity results analyzed and presented here, we manually proofread all predicted pre- and postsynapses of the 40 core T4 and T5 neurons as well as the dendrite fragments of the HS and VS cells (Figure 3) and the bilayer LPI cells (Figure 4) for higher quality results. Neurons and synapses were proofread and visualized using the NeuTu⁷⁰ software package.

After identifying representative T4 and T5 cells, five cells per each subtype, their synaptic partners in the lobula plate were exhaustively traced, though not necessarily to completion. Most of the cells documented in previous studies, including prominent LPTCs, were identified by their morphology. When two or more neurons have similar morphology, information of the spatial distributions of pre- and postsynaptic terminals, synapse counts, as well as the neuron types sharing synaptic connections were used to determine the cell types. New neuron types identified in this work (part of Figures 5 and 6) were named following the nomenclature convention of the optic lobe neurons primarily introduced by Fischbach and Dittrich.¹⁶ The lobula plate tangential cells (LPTCs) have traditionally been given unique names, such as the HS, VS, and CH cells. Newly found LPTCs were distinguished by the extent of branching arbors in the lobula plate. Using a similar format used by Fischbach and Dittrich¹⁶ and Otsuna and Ito⁷² for other neuron types, we tentatively named these cells by combining LPT (lobula plate tangential) + innervating layers + alphabetical identifier, e.g., LPT3b and LPT34a. This nomenclature aligns with neuron names such as the lobula tangential (LT), medulla tangential (MT), and lobula columnar (LC) cells, while using “C” for “cell” was avoided for naming individual neurons as it is commonly used to abbreviate “columnar”. Likewise, the names for the columnar lobula plate cells, LPC, LLPC, and LPLC, match the names used in other studies carried out at the Janelia Research Campus.^{43,48,49} Neurons were given tentative names as far as the overall morphology was reconstructed or, at least, a characteristic branch in the lobula plate was sufficiently reconstructed (in the case of LPI and LPTCs). Numbers used in the names of the Tlp and Y cells were selected to avoid overlap with numbers in Fischbach and Dittrich¹⁶ (since EM/Golgi matches can be inclusive). Gaps in the numbering of TmY neuron types reflect cell types identified in ongoing work that are not T4 or T5 synaptic partners by the criteria used in this study and therefore are not included here. In contrast to the bilayer LPI names, the names of the TmY, Tlp, Y cells, etc. do not refer to the lobula plate layer pattern of these neurons.

Light microscopy (LM) and LM/EM comparison

Individual cells were labeled using MultiColorFlpOut (MCFO).¹⁸ Details of the fly crosses for each supporting figure panel are listed in Table S1. All images show cells from female flies. Images were acquired on Zeiss LSM 710 or 780 confocal microscopes with 63×1.4 NA objectives at $0.19 \mu\text{m} \times 0.19 \mu\text{m} \times 0.38 \mu\text{m}$ or $0.38 \mu\text{m} \times 0.38 \mu\text{m} \times 0.38 \mu\text{m}$ voxel size. Samples were prepared and imaged by the Janelia FlyLight Project Team. Detailed protocols are available online (<https://www.janelia.org/project-team/flylight/protocols>). We used GAL4 lines from the Janelia and Vienna Tiles collections.^{12,19} Figures show views of substacks rendered using VVD viewer (https://github.com/takashi310/VVD_Viewer). In some cases, additional labeled cells or background signal were removed by manual editing in VVD viewer. Original confocal stacks are available online as part of the Janelia FlyLight MCFO collection at http://gen1mcfo.janelia.org/cgi-bin/view_gen1mcfo_imaging.cgi?slidecode=slidecode. Use this link with the appropriate slide code from Table S1 replacing *slidecode* and select “Download LSM” (or ‘Download unaligned stack’ for stitched multi-tile images) under “Select a product to view”.

LM and EM matches are based on visually comparing anatomical features, in particular cell body location and arborizations in specific optic lobe subregions and layers (Figures S2 and S3). With the exception of LPI2c and LPI3a (which we did not attempt to match due to their comparatively few distinct features and small size) and LPI2-1 (for which we did not identify LM images), we confirmed the cell shapes of all newly identified optic lobe intrinsic cell types by identifying probable light microscopy matches.

QUANTIFICATION AND STATISTICAL ANALYSIS

Both automatically predicted and manually proofread synapses of reconstructed neurons were counted on NeuTu.⁷⁰ The neuronal connectivity diagrams (Figures 2A and S1) were generated using Cytoscape (<https://cytoscape.org/>) software. In the figures and the main text, the numbers of synaptic connections are averaged among the core neurons (five cells per each subtype) for T4 and T5, while raw numbers are shown for other neuron types. The raw data of the synaptic connections are provided as Data S1, S2, and S3.

Current Biology, Volume 32

Supplemental Information

Neuronal circuits integrating visual motion

information in *Drosophila melanogaster*

Kazunori Shinomiya, Aljoscha Nern, Ian A. Meinertzhagen, Stephen M. Plaza, and Michael B. Reiser

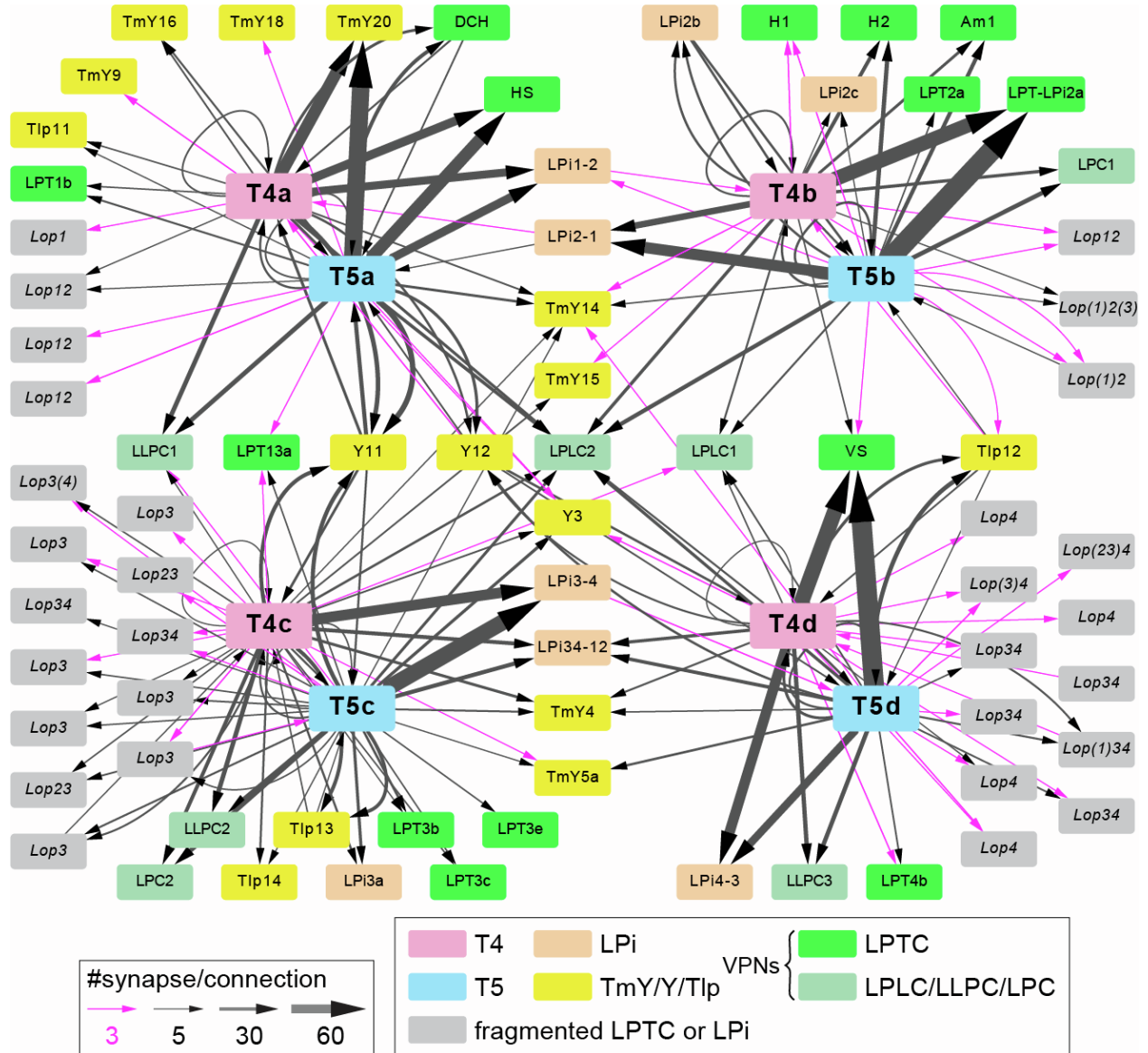


Figure S1. The inputs and outputs of representative T4 and T5 cells in the lobula plate (more than three synapse). Related to Figure 2.

Inputs and outputs corresponding to a mean of more than three synapses per T4 or T5 cell are shown in the diagram, in contrast to a threshold of five synapses used in Figure 2A. Connections with more than three and less than five mean synapses are shown with magenta arrows. By lowering the threshold, the number of unidentifiable fragmented cells (shown in gray) increased from 16 to 30, while only three identified neuron types (TmY9 and TmY18 in Lop1, and H1 in Lop2) are newly included in this summary connectivity diagram (based on data in Data S1).

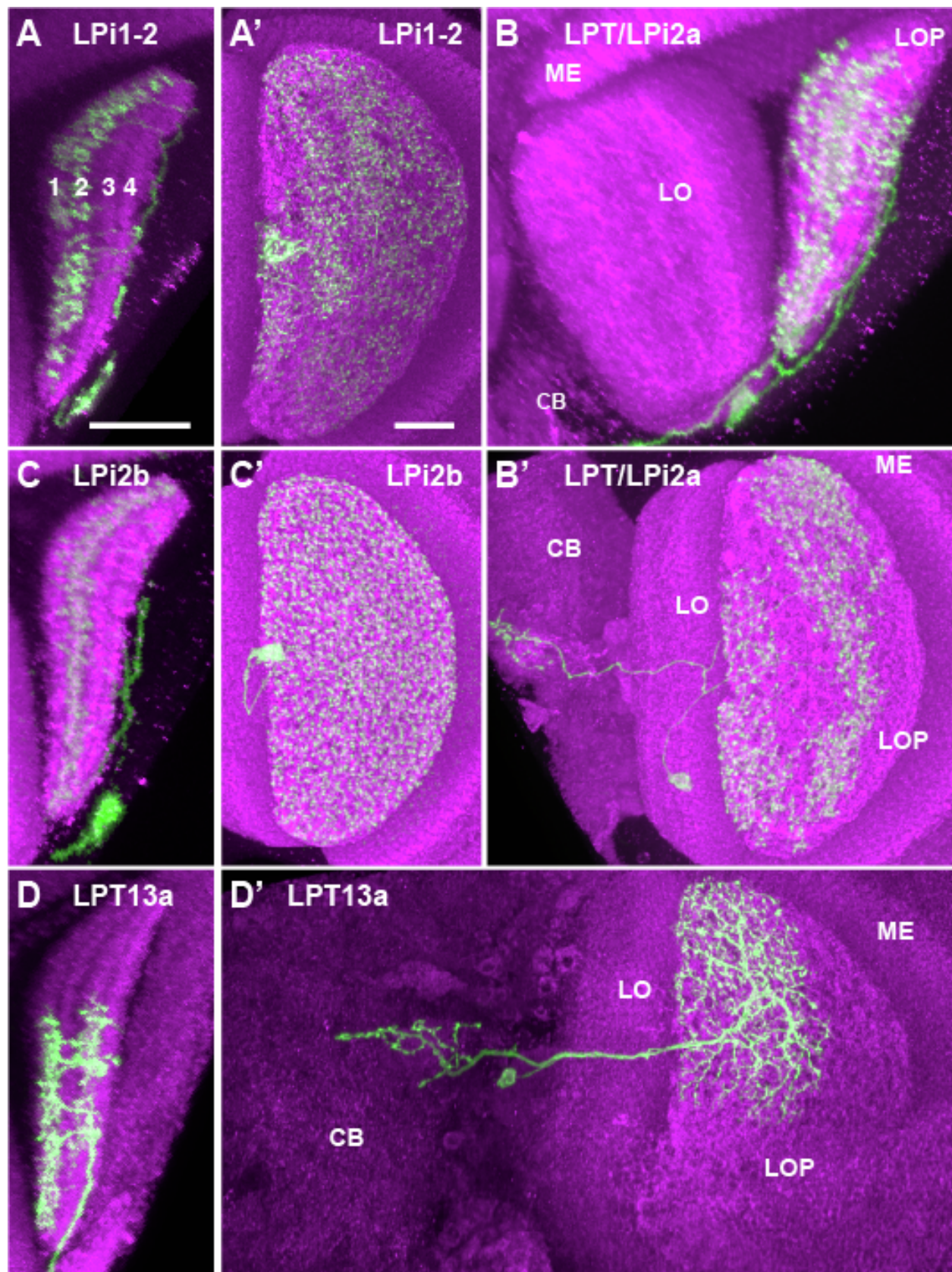


Figure S2. Candidate light microscopy matches for large LPi-like cells. Related to Figure 6.
Images show resampled views generated from confocal stacks with MCFO-labeled neurons using VVD viewer (see Methods). Some images were manually edited in VVD viewer in order to only show the cells of interest. Panels show either the lobula plate layers (in a view similar to Figures 5 and 6) (A, B, C, and D) or an *en face* view of the lobula plate from posterior (A', B', C', and D'). Cell type names indicate apparent EM matches. Scale bars in A and A' represent 20 μm . Other panels are shown at similar but not identical scale. Note that the neuropils appear to be much smaller than those in the EM sample (e.g., Figure 1A) due to shrinkage from dehydration for DPX mounting (see Methods and also Figure 19 of Scheffer et al.^{S1}). Numbers in panel A mark lobula plate layers. Brains regions are indicated in (B, B', and D') (CB, central brain).

(A) A large lobula plate intrinsic cell that locally matches the arbor structure (thin processes, likely dendritic in Lop1, varicosities, likely presynaptic, in Lop2; parallel processes to and soma in the lobula plate cell body rind) of LPi1-2 (Figure 4). (A') Arbor spread of the neuron in (A). Processes cover most of the lobula plate in a non-uniform pattern. (B) Layer pattern and lobula plate coverage (B') of a neuron resembling LPT/LPi2a (Figure 6B). Central projection suggests that the neuron we identify in the EM volume as LPT/LPi2a is likely a VPN. (C) Layer pattern of an apparent LM match of LPi2b (Figure 6C). This cell covers all of the lobula plate (C'). (D) A lobula plate tangential cell matching the arborization pattern of LPT13a. The cell innervates the Lop1 and Lop3 layers, where it receives weak inputs from T5a, T4c, and T5c (Figure S1). The cell terminates in the central brain (D') with a presumptive presynaptic terminal.

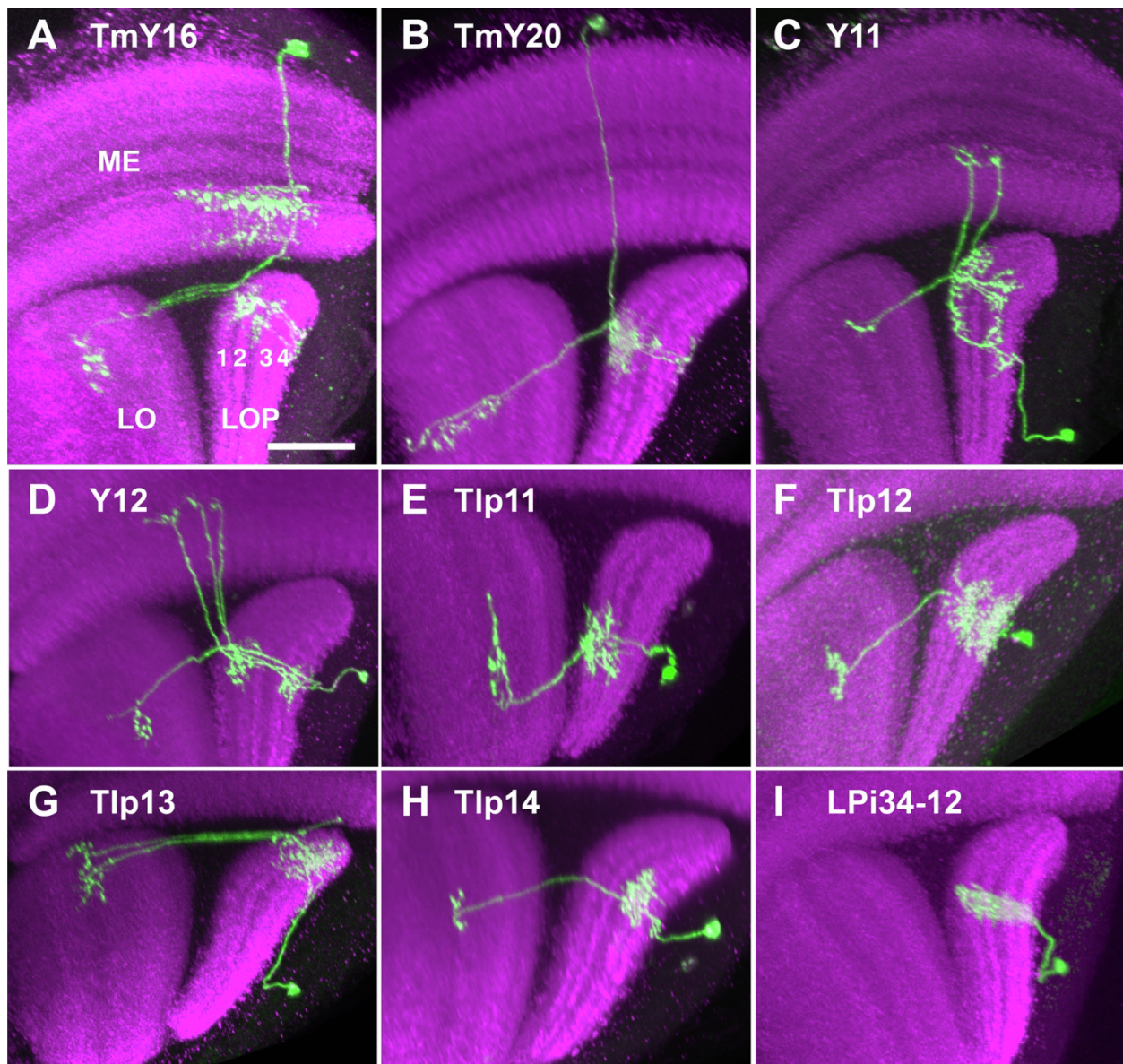


Figure S3. Candidate light microscopy matches for newly described optic lobe intrinsic cell types. Related to Figure 6.

Images show resampled views generated from confocal stacks with MCFO-labeled neurons using VVD viewer (see Methods). Some images were manually edited in VVD viewer in order to only show the cells of interest. Panels show the lobula plate layers (displayed in a view similar to Figures 5 and 6). Cell type names indicate apparent EM matches. Scale bar in A represent 20 μm . Other panels are shown at similar but not identical scale. Numbers in panel A mark lobula plate layers, optic lobe regions as indicated. (A) TmY16, (B) TmY20, (C) Y11, (D) Y12, (E) Tlp11, (F) Tlp12, (G) Tlp13, (H) Tlp14, (I) LPi34-12.

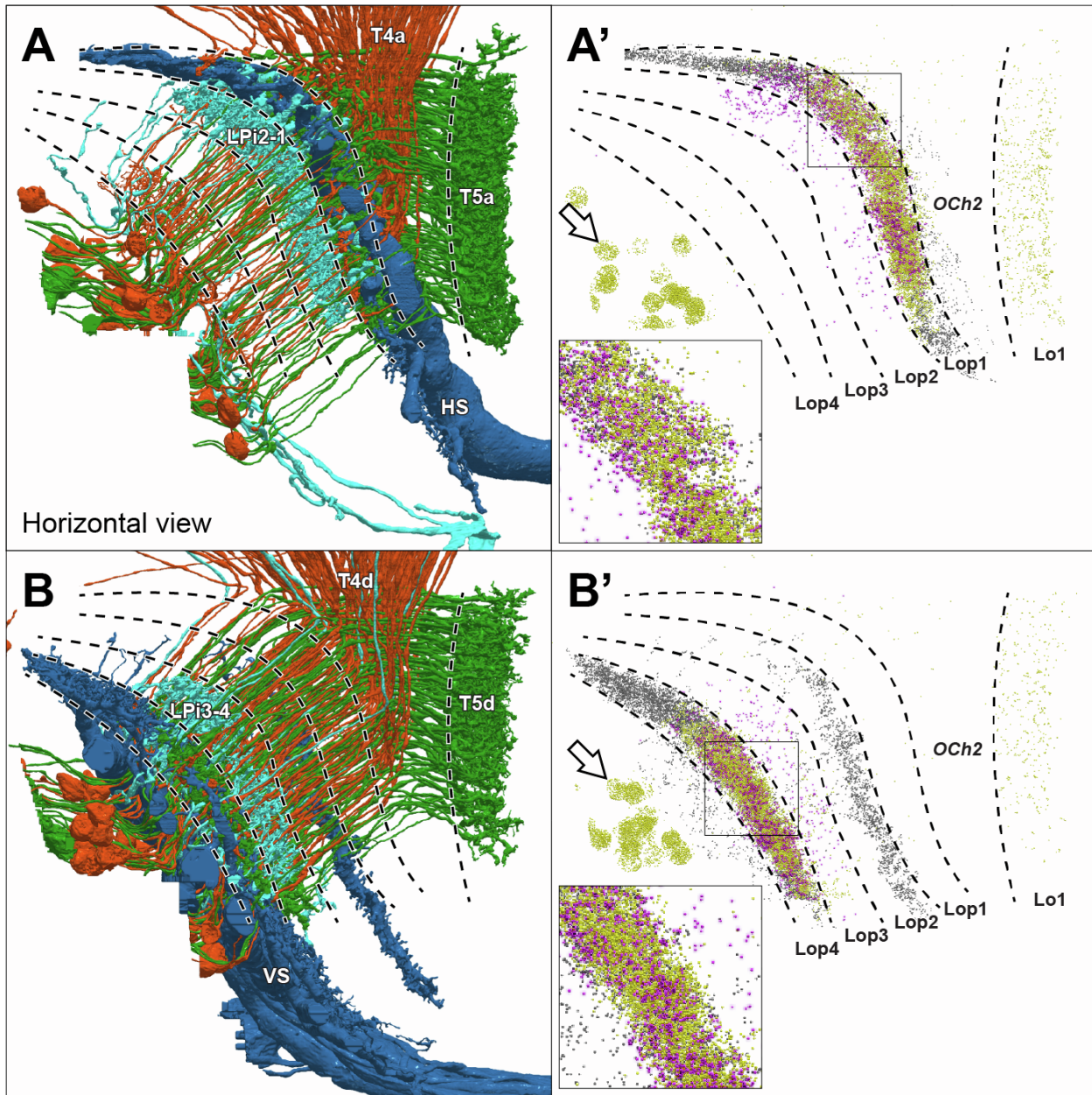


Figure S4. HS, VS cells and their input neurons. Related to Figure 3.

(A) Neurons and their synapses in Lop1, including HSE, HSN and HSS, fully reconstructed T4a and T5a (mostly populated around the center of the neuropil), and LPi2-1. In A', postsynapses of HS (gray), presynapses of T4a and T5a (yellow), presynapses of LPi2-1 (magenta) are shown.

(B) Neurons and their synapses in Lop4, including 10 VS and VS-like cells, fully reconstructed T4d and T5d, and LPi3-4 cells. In B', postsynapses of VS (gray), presynapses of T4d and T5d (yellow), presynapses of LPi3-4 (magenta) are shown. The synapses shown include predicted (not proofread) synapses. Synapses on the T4/T5 cell bodies outside of the Lop4 layer (arrows) appear to be false-positive predictions.

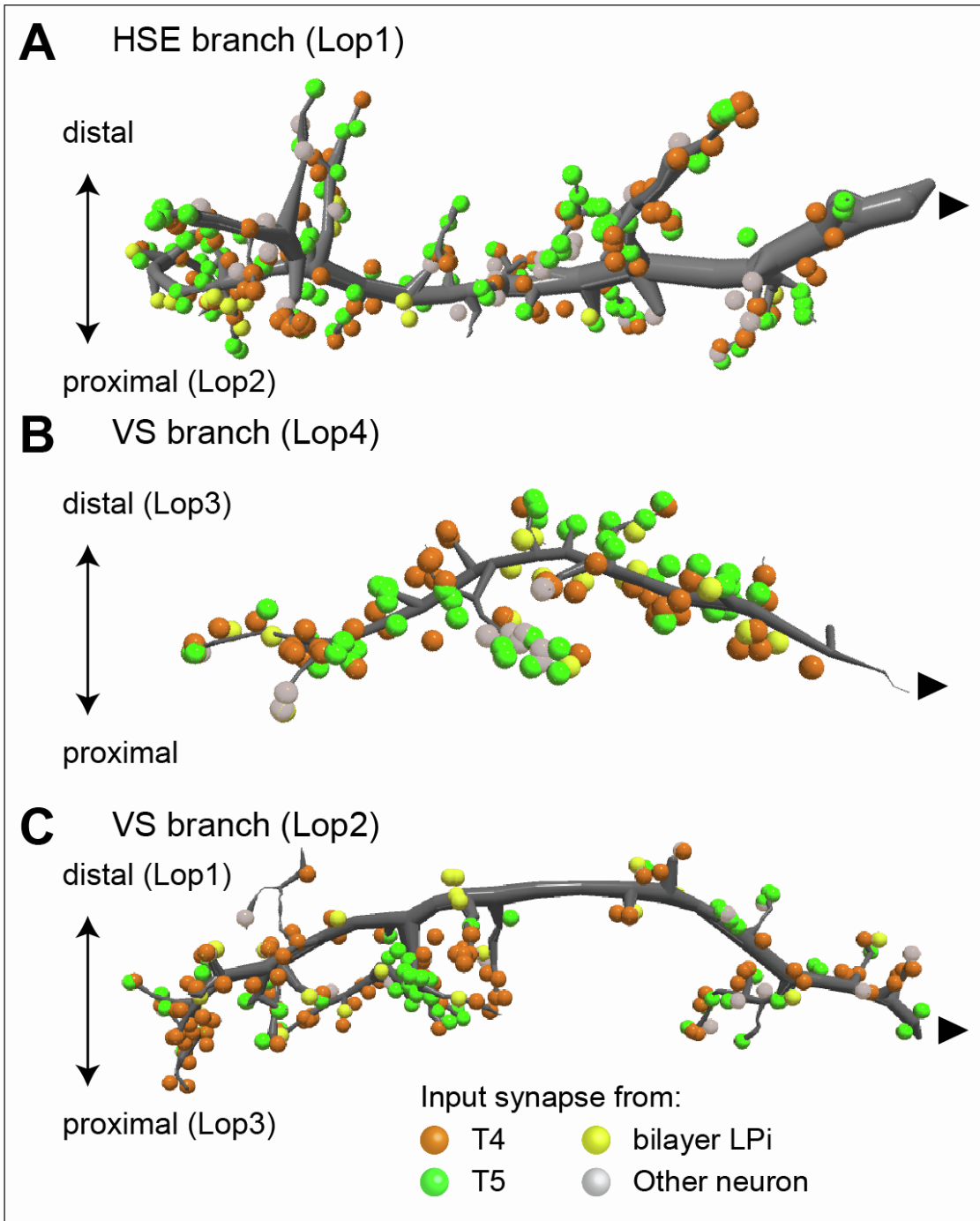


Figure S5. Distribution of input synapses on HS and VS cell branches. Related to Figure 3.
 Synapse distributions on an HSE cell branch in Lop1 (A), VS cell branches in Lop4 (B) and Lop2 (C), projected horizontally. Each dot represents a single input synapse on the skeletonized cell branches; orange, green, yellow, and gray dots indicate inputs from T4, T5, bilayer LPi cells, and other cell types, respectively. Some synapses appear to be detached from the neurons because of approximate skeletonization of the branches. Arrowheads show the roots of the cell branches connecting to the rest of each neuron. On each branch, inputs from the major cell types appear to be randomly distributed regardless of the cell types and the depth in the layers.

Figure panel(s)	Fly cross	Slide code for download of original image stacks (see Methods)
S2A, S2A'	R20F11-GAL4 crossed to MCFO-7 (Nern, et al. 2015 ^{S2})	20140508_32_E6
S2B, S2B'	R15D05-Gal4 crossed to MCFO-7	20130429_2_B2
S2C, S2C'	R42B05-GAL4 crossed to MCFO-7	20130529_1_D2
S2D, S2D'	R11D02-GAL4 crossed to MCFO-7	20140701_19_H3
S3A, S3C, S3D, S3I	OL-KD (29C07-KDGeneswitch-4) in attP40; R57C10-GAL4 in attP2 tubP-KDRT>GAL80-6-KDRT> in VK00027 crossed to MCFO-1 (Nern, et al. 2015 ^{S2})	20120222_2_B2 (S3A) 20120224_1_G1 (S3C) 20120507_1_A2 (S3D) 20120111_5_E5 (S3I)
S3B	VT048842-GAL4 crossed to MCFO-7	20140207_33_F3
S3E	R10E08-GAL4 crossed to MCFO-7	20130410_2_B5
S3F	R87B02-GAL4 crossed to MCFO-7	20120731_1_C3
S3G	VT016795-GAL4 crossed to MCFO-7	20131010_31_C8
S3H	VT016279-GAL4 crossed to MCFO-7	20131004_34_B3

Table S1: Fly crosses used to visualize lobula plate neurons in this study and image identifiers by figure panel. Related to the STAR Methods.

Supplemental References

- S1. Scheffer, L.K., Xu, C.S., Januszewski, M., Lu, Z., Takemura, S.Y., Hayworth, K.J., Huang, G.B., Shinomiya, K., Maitlin-Shepard, J., Berg, S., *et al.* (2020). A connectome and analysis of the adult *Drosophila* central brain. *eLife* 9. 10.7554/eLife.57443.
- S2. Nern, A., Pfeiffer, B.D., and Rubin, G.M. (2015). Optimized tools for multicolor stochastic labeling reveal diverse stereotyped cell arrangements in the fly visual system. *Proc Natl Acad Sci U S A* 112, E2967-2976. 10.1073/pnas.1506763112.